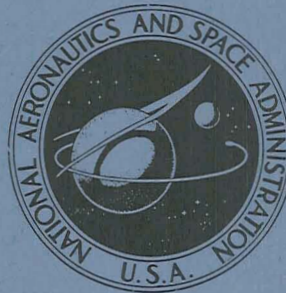


N71-31254

NASA TECHNICAL
MEMORANDUM



NASA TM X-2341

NASA TM X-2341

CASE FILE
COPY

SUBSONIC STABILITY, CONTROL, AND
PERFORMANCE OF A SHUTTLE CONCEPT
WITH A BLENDED WING-BODY



by Charles H. Fox, Jr., and Delma C. Freeman, Jr.

Langley Research Center

Hampton, Va. 23365

1. Report No. NASA TM X-2341	2. Government Accession No.	3. Recipient's Catalog No.	
4. Title and Subtitle SUBSONIC STABILITY, CONTROL, AND PERFORMANCE OF A SHUTTLE CONCEPT WITH A BLENDED WING-BODY		5. Report Date July 1971	
		6. Performing Organization Code	
7. Author(s) Charles H. Fox, Jr., and Delma C. Freeman, Jr.		8. Performing Organization Report No. L-7682	
		10. Work Unit No. 117-07-01-01	
9. Performing Organization Name and Address NASA Langley Research Center Hampton, Va. 23365		11. Contract or Grant No.	
		13. Type of Report and Period Covered Technical Memorandum	
12. Sponsoring Agency Name and Address National Aeronautics and Space Administration Washington, D.C. 20546		14. Sponsoring Agency Code	
15. Supplementary Notes			
16. Abstract <p>An investigation has been conducted in the Langley high-speed 7- by 10-foot tunnel to determine the longitudinal and lateral-directional aerodynamic characteristics of a model representative of a high-cross-range orbiter with a blended delta wing-body at subsonic speeds. The model had a leading-edge sweep of 67.5° and tip fins having 5° toe-in and 15° roll-out. The model was tested over a Mach number range from 0.4 to 0.88 at angles of attack from approximately -4° to 20°.</p> <p>The results of the investigation indicate that at low-subsonic Mach numbers the model, with the moment center at 66.7 percent of the body length, is stable up to an angle of attack of 11°, where a slight pitch-up occurs. Increasing the Mach number to 0.8 delays this pitch-up until an angle of attack of 18° is reached. Large elevon deflections were required to trim the model because of the large negative values of zero-lift pitching moment and the low elevon effectiveness. The resulting values of trimmed lift and trimmed lift-to-drag ratio were undesirably low. Removing the fuselage boattailing and tip-fin camber decreased the negative zero-lift pitching moment slightly; however, there was no net gain in performance. The model was directionally stable and had positive effective dihedral at the lowest Mach number, but increasing the Mach number to 0.8 resulted in a loss of directional stability.</p>			
17. Key Words (Suggested by Author(s)) Space shuttle vehicles Blended delta wing-body		18. Distribution Statement Unclassified - Unlimited	
19. Security Classif. (of this report) Unclassified	20. Security Classif. (of this page) Unclassified	21. No. of Pages 45	22. Price* \$3.00

SUBSONIC STABILITY, CONTROL, AND PERFORMANCE OF A SHUTTLE CONCEPT WITH A BLENDED WING-BODY

By Charles H. Fox, Jr., and Delma C. Freeman, Jr.
Langley Research Center

SUMMARY

An investigation has been conducted in the Langley high-speed 7- by 10-foot tunnel to determine the longitudinal and lateral-directional aerodynamic characteristics of a model representative of a high-cross-range orbiter with a blended delta wing-body at subsonic speeds. The model had a leading-edge sweep of 67.5° and tip fins having 5° toe-in and 15° roll-out. The model was tested over a Mach number range from 0.4 to 0.88 at angles of attack from approximately -4° to 20° .

The results of the investigation indicate that at low-subsonic Mach numbers the model, with the moment center at 66.7 percent of the body length, is stable up to an angle of attack of 11° , where a slight pitch-up occurs. Increasing the Mach number to 0.8 delays this pitch-up until an angle of attack of 18° is reached. Large elevon deflections were required to trim the model because of the large negative values of zero-lift pitching moment and the low elevon effectiveness. The resulting values of trimmed lift and trimmed lift-to-drag ratio were undesirably low. Removing the fuselage boattailing and tip-fin camber decreased the negative zero-lift pitching moment slightly; however, there was no net gain in performance. The model was directionally stable and had positive effective dihedral at the lowest Mach number, but increasing the Mach number to 0.8 resulted in a loss of directional stability.

INTRODUCTION

One of the current goals of the National Aeronautics and Space Administration is the development of a space transportation system capable of placing large payloads in near-earth orbit. As part of this general effort, wind-tunnel tests of a scale model of a typical high-cross-range orbiter concept with a blended delta wing-body, have recently been made at Langley Research Center. The present investigation conducted in the Langley high-speed 7- by 10-foot tunnel consisted of tests to determine the basic subsonic longitudinal and lateral-directional aerodynamic characteristics of the model. The model was tested over a range of Mach numbers from 0.4 to 0.88 corresponding to Reynolds numbers, based on body length, of 5×10^6 to 8×10^6 , respectively, and at angles

of attack from approximately -4° to 20° at 0° of sideslip. The model was also tested at angles of attack of 0° and 9° through a range of sideslip angles from -4° to 10° .

SYMBOLS

The longitudinal data are referred to the stability system of axes, and the lateral-directional data are referred to the body system of axes. (See fig. 1.) The moment reference center was located at 66.7 percent of the body length.

b	reference wing span, 35.66 cm
C_D	drag coefficient, $\frac{\text{Drag}}{qS}$
$C_{D,b}$	base-drag coefficient, $\frac{\text{Base drag}}{qS}$
C_L	lift coefficient, $\frac{\text{Lift}}{qS}$
C_l	rolling-moment coefficient, $\frac{M_X}{qSb}$
C_m	pitching-moment coefficient, $\frac{M_Y}{qS}$
$C_{m,0}$	pitching-moment coefficient at $C_L = 0$
C_n	yawing-moment coefficient, $\frac{M_Z}{qSb}$
C_Y	side-force coefficient, $\frac{\text{Side force}}{qS}$
D	drag force, newtons
F_Y	side force, newtons
L	lift force, newtons
l	body length, 66.26 cm
M	Mach number
M_X	rolling moment, m-N

M_Y	pitching moment, m-N
M_Z	yawing moment, m-N
q	dynamic pressure, N/m ²
S	total planform area, 0.121 m ²
X, Y, Z	body reference axes
x, y	coordinates along X- and Y-axis, respectively
α	angle of attack, deg
β	angle of sideslip, deg
ΔC_l	incremental rolling-moment coefficient due to control deflection
ΔC_n	incremental yawing-moment coefficient due to control deflection
ΔC_Y	incremental side-force coefficient due to control deflection
δ_e	elevon deflection, positive when trailing edge is down, deg
δ_r	rudder deflection, positive when trailing edge is deflected to left, deg
ψ	angle of yaw, deg

Subscripts:

L	left control surface
R	right control surface
s	stability axes

DESCRIPTION OF MODEL

The model tested was an approximately 0.013-scale model of a high-cross-range orbiter concept. The general arrangement of the model is shown in figure 2(a); wing

cross section, afterbody details, and vertical-tail cross sections are presented in figures 2(b), 2(c), and 2(d), respectively. A photograph of the model mounted in the test section of the Langley high-speed 7- by 10-foot tunnel is presented in figure 3. The model had a leading-edge sweep of 67.5° and outboard-mounted fins having 5° toe-in and 15° roll-out. Elevon surfaces functioned both for pitch control and roll control, and rudders on the tip fins functioned for directional control.

APPARATUS, TESTS, AND CORRECTIONS

The present investigation was conducted in the Langley high-speed 7- by 10-foot tunnel. Forces and moments were measured with a sting-supported, internally mounted, six-component strain-gage balance. Tests were made at Mach numbers from 0.4 to 0.88 corresponding to free-stream Reynolds numbers, based on model length, of 5×10^6 to 8×10^6 . The angle-of-attack range was from approximately -4° to 20° at a sideslip angle of 0° . Tests were also run at angles of attack of 0° and 9° through an angle-of-sideslip range from approximately -4° to 10° . The data have been corrected for blockage and jet-boundary effects by the methods of references 1 and 2. Angles of attack have been corrected for the effects of balance and sting deflection due to aerodynamic load. Chamber-pressure measurements were made for all configurations, and the corresponding base drag was computed and is presented in part (c) of figures 4 to 7 and 9; however, the basic data presented in part (b) of figures 4 to 7 and 9 are uncorrected for the effects of base drag. For the configuration with the modified afterbody, base-pressure measurements were made in addition to the chamber-pressure measurements and were included in the base-drag calculations presented in figure 9(c). All tests were made with transition fixed on the model by means of a 0.254-cm-wide strip of No. 100 carborundum grit located 2.54 cm behind the leading edge of the wing and 2.54 cm behind the nose. (See ref. 3.)

PRESENTATION OF DATA

	Figure
Effect of Mach number on longitudinal aerodynamic characteristics of model. $\delta_e = 0^\circ$	4
Effect of Mach number on longitudinal aerodynamic characteristics of model. $\delta_e = -30^\circ$	5
Longitudinal-control effectiveness. $M = 0.4$	6
Longitudinal-control effectiveness. $M = 0.8$	7
Trim-performance characteristics of basic model. $M = 0.4$	8
Effect of afterbody and tip-fin modifications on longitudinal aerodynamic characteristics of model. $\delta_e = 0^\circ$; $M = 0.4$	9

	Figure
Static lateral stability characteristics of model. $\delta_e = 0^\circ$	10
Roll-control effectiveness, asymmetric elevon deflection for roll control	11
Combined roll- and yaw-control effectiveness	12

RESULTS AND DISCUSSION

Static Longitudinal Stability and Control

Effects of Mach number.- The longitudinal aerodynamic characteristics of the model with the elevon surfaces undeflected are presented in figure 4 for the test Mach number range from 0.4 to 0.88. These data show that the model was statically longitudinally stable up to about 11° angle of attack in the low Mach number range; however, increasing the Mach number to 0.80 resulted in the longitudinal stability being maintained up to an angle of attack of 18° , where a pronounced instability occurred. The longitudinal instability at angles of attack above 18° for the highest Mach number probably resulted from changes in the lift distribution over the wing-body combination due to trailing-edge separation. The data of figure 5 present the results of tests to determine the effects of Mach number on the longitudinal aerodynamic characteristics with the elevon surface deflected upward 30° . The trends of these data are similar to those of the data of figure 4. It should be noted, however, that a comparison of the data of figures 4 and 5 indicates that as the Mach number is increased, the longitudinal-control effectiveness is reduced. This effect is not uncommon for trailing-edge controls on relatively thick wings. The presence of the vertical fins at the wing tips would be expected to further aggravate this problem, such as the case of reference 4.

Longitudinal-control effectiveness.- The data for longitudinal-control effectiveness of figures 6 and 7 show that large elevon deflections are required to trim the model because of the large negative values of $C_{m,o}$ and low values of elevon effectiveness. A similar effect was noted in reference 5. The values of $(L/D)_{trim}$ and $(C_L)_{trim}$ are presented in figure 8. These data show that the largest deflection tested was required to trim the model at the higher angles of attack and resulted in very low values of $(L/D)_{trim}$ and $(C_L)_{trim}$.

Effect of afterbody modification.- The data of figure 9 present the results of tests to determine the effects of altering the afterbody (see fig. 2(c)) on the large negative $C_{m,o}$ and, therefore, on the low $(L/D)_{trim}$ of the model. The data show that altering the afterbody resulted in a small decrease in the negative $C_{m,o}$, but any reduction in the trim drag was offset by an increase in base drag so that there was probably no net gain in $(L/D)_{trim}$ and $(C_L)_{trim}$.

Static Lateral Stability and Control

Lateral stability characteristics.- The static lateral stability characteristics are presented in figure 10. These data show that for the two angles of attack tested (0° and 9°) for a range of sideslip angles of about $\pm 4^\circ$ the lateral coefficients were linear. The data for a Mach number of 0.4 (fig. 10(a)) show that the model was directionally stable and had positive effective dihedral at both angles of attack tested. Increasing the Mach number to 0.8 (fig. 10(b)) resulted in a loss of directional stability and an effective dihedral of near zero. This result has been observed in previous tests (ref. 4) and is associated with the loss of the effectiveness of the tip fins because of trailing-edge separation on the wing.

Lateral-control effectiveness.- Data showing the effectiveness of asymmetric elevon deflection for roll control are presented in figure 11. The data measured at a Mach number of 0.4 (fig. 11(a)) show that the elevons were effective for roll control even at a trim deflection of -40° . Increasing the Mach number to 0.8 resulted in a slight increase in roll-control effectiveness; however, there was some adverse yaw at this Mach number.

Data for coordinated lateral-directional control are presented in figure 12. The rudder was deflected in combination with the roll control in order to eliminate any adverse roll associated with the rudder deflection. The data show that the rudder was effective for yaw control throughout the test angle-of-attack range, and at the highest rudder deflection (-20°), an elevon deflection of 10° was more than adequate to eliminate adverse roll. At the highest Mach number (0.8), no adverse roll was associated with the rudder deflection.

SUMMARY OF RESULTS

The results of an investigation to determine the subsonic aerodynamic characteristics of an orbiter with a blended delta wing-body may be summarized as follows:

1. The results of the investigation indicate that at low-subsonic Mach numbers the model, with the moment center at 66.7 percent of the body length, is stable up to an angle of attack of 11° , where a slight pitch-up occurs. Increasing the Mach number to 0.8 delays this pitch-up until an angle of attack of 18° is reached.

2. Large elevon deflections were required to trim the model because of the large negative values of zero-lift pitching moment and the low elevon effectiveness. The resulting values of trimmed lift and trimmed lift-to-drag ratio were undesirably low.

3. Removing the fuselage boattailing and tip-fin camber decreased the negative zero-lift pitching moment slightly; however, any decrease in trim drag was offset by an increase in base drag.

4. The model was directionally stable and had positive effective dihedral at the lowest Mach number, but increasing the Mach number to 0.8 resulted in a loss of directional stability and nearly zero effective dihedral.

5. Asymmetric elevon deflections were effective for roll control at both Mach numbers about pitch-trim deflections as high as -40° .

6. Overall, the results indicate that this configuration has undesirable aerodynamic characteristics.

Langley Research Center,
National Aeronautics and Space Administration,
Hampton, Va., June 25, 1971.

REFERENCES

1. Herriot, John G.: Blockage Corrections for Three-Dimensional-Flow Closed-Throat Wind Tunnels, With Consideration of the Effect of Compressibility. NACA Rep. 995, 1950. (Supersedes NACA RM A7B28.)
2. Gillis, Clarence L.; Polhamus, Edward C.; and Gray, Joseph L., Jr.: Charts for Determining Jet-Boundary Corrections for Complete Models in 7- by 10-Foot Closed Rectangular Wind Tunnels. NACA WR L-123, 1945. (Formerly NACA ARR L5G31.)
3. Braslow, Albert L.; Hicks, Raymond M.; and Harris, Roy V., Jr.: Use of Grit-Type Boundary-Layer-Transition Trips on Wind-Tunnel Models. NASA TN D-3579, 1966.
4. McKinney, Linwood W.; and Huffman, Jarrett K.: Subsonic Aerodynamic Characteristics of a Model of the HL-10 Flight Research Vehicle With Basic and Modified Tip Fins. NASA TM X-2119, 1971.
5. Freeman, Delma C., Jr.: Low-Subsonic Aerodynamic Characteristics of a Space Shuttle-Orbiter Concept With a Blended Delta Wing-Body. NASA TM X-2209, 1971.

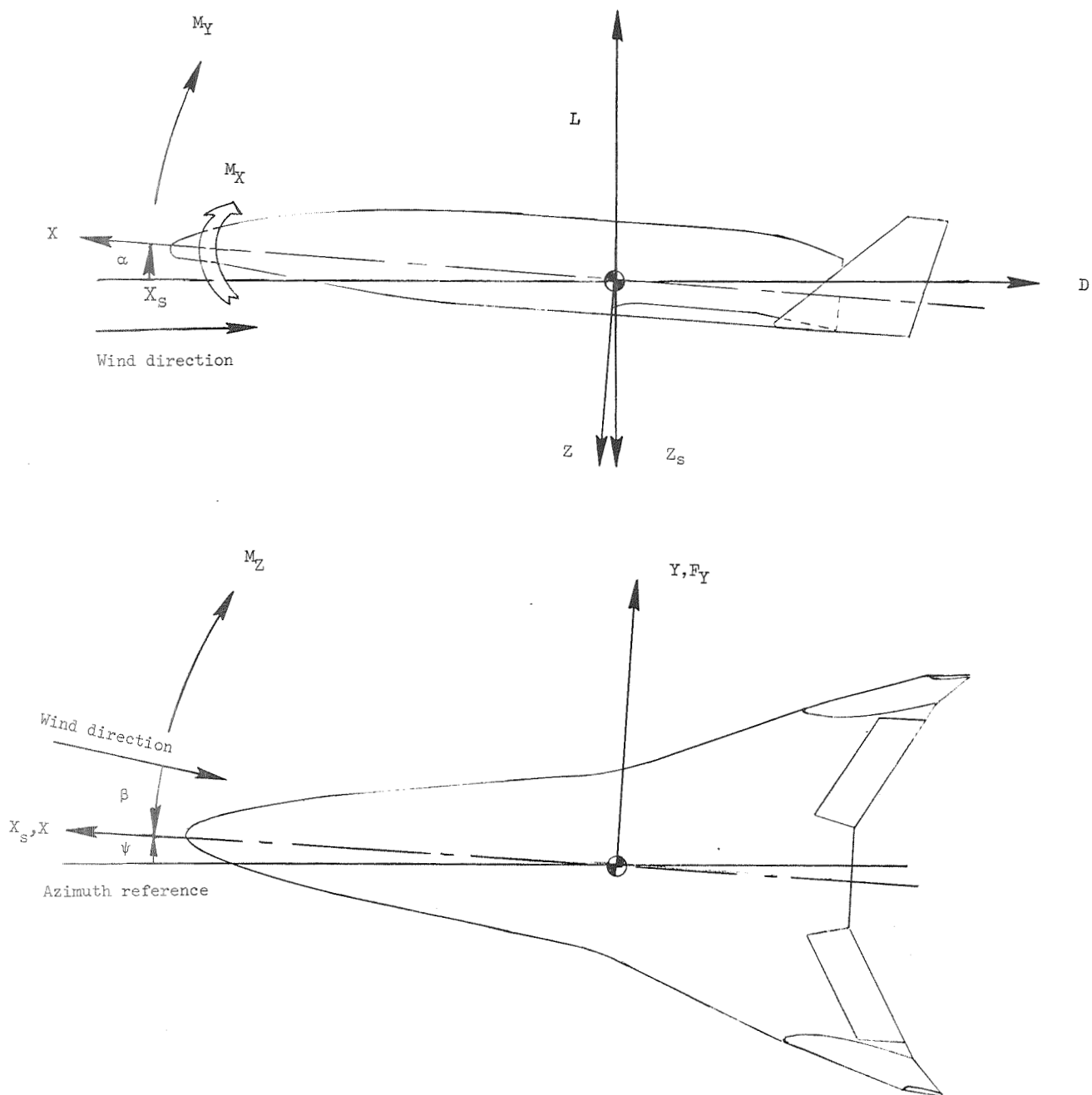


Figure 1.- System of axes used in investigation. Arrows indicate positive directions of moments, forces, and angles.

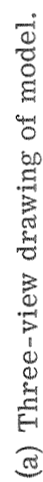
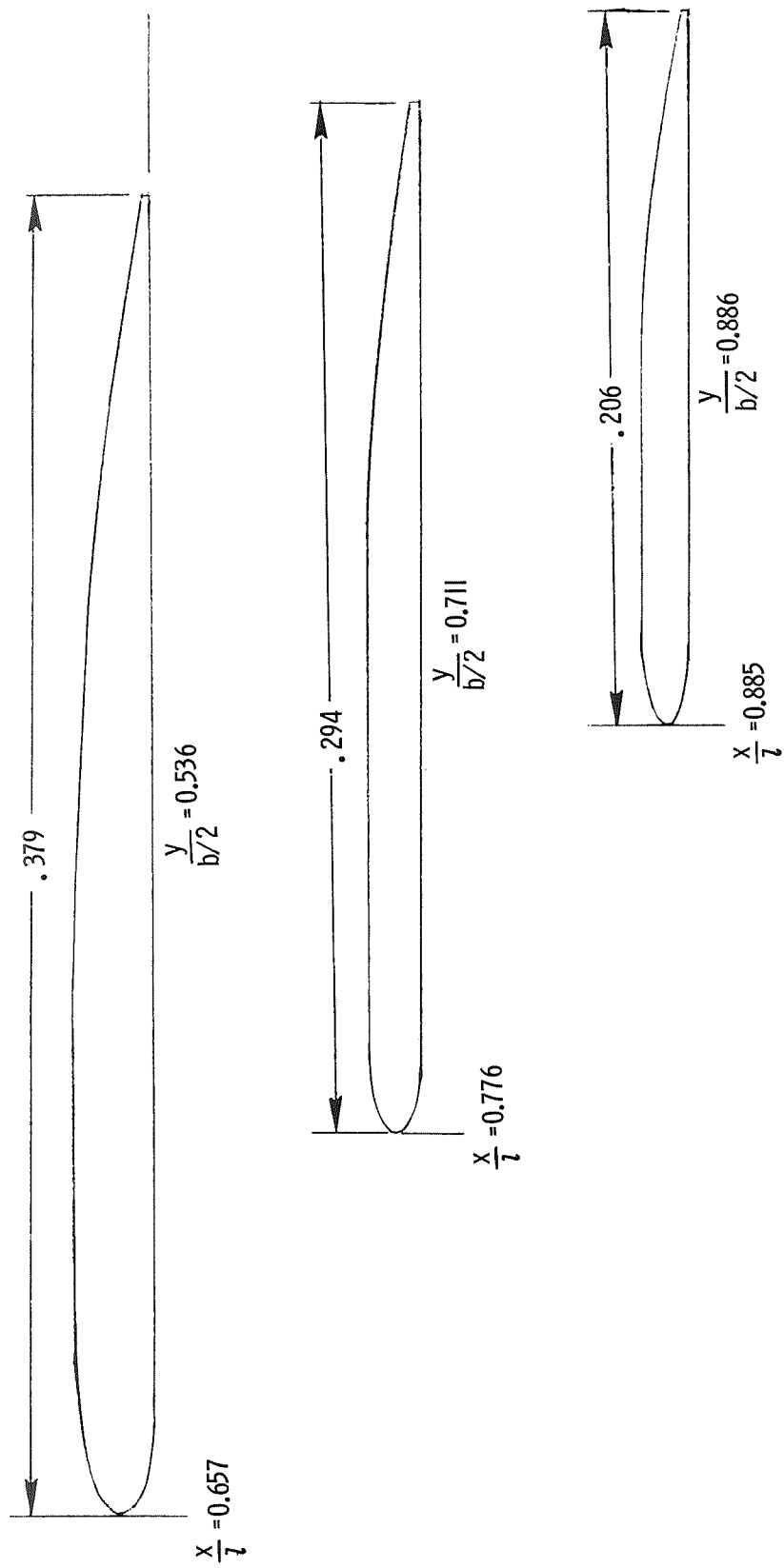
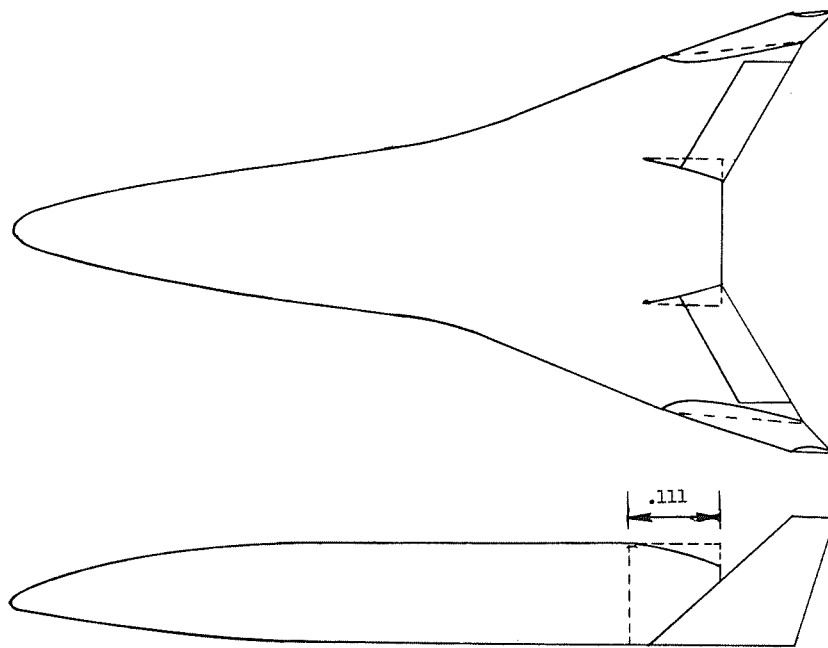


Figure 2.- Detail drawings of model. Linear dimensions are based on a body length l of 66.26 cm (26.087 inches) unless otherwise noted.

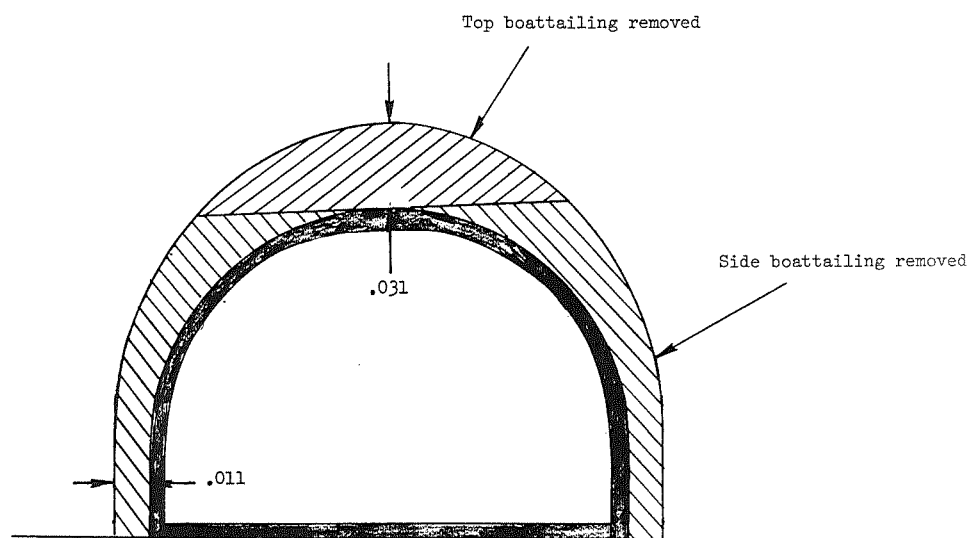


(b) Wing cross sections.

Figure 2.- Continued.



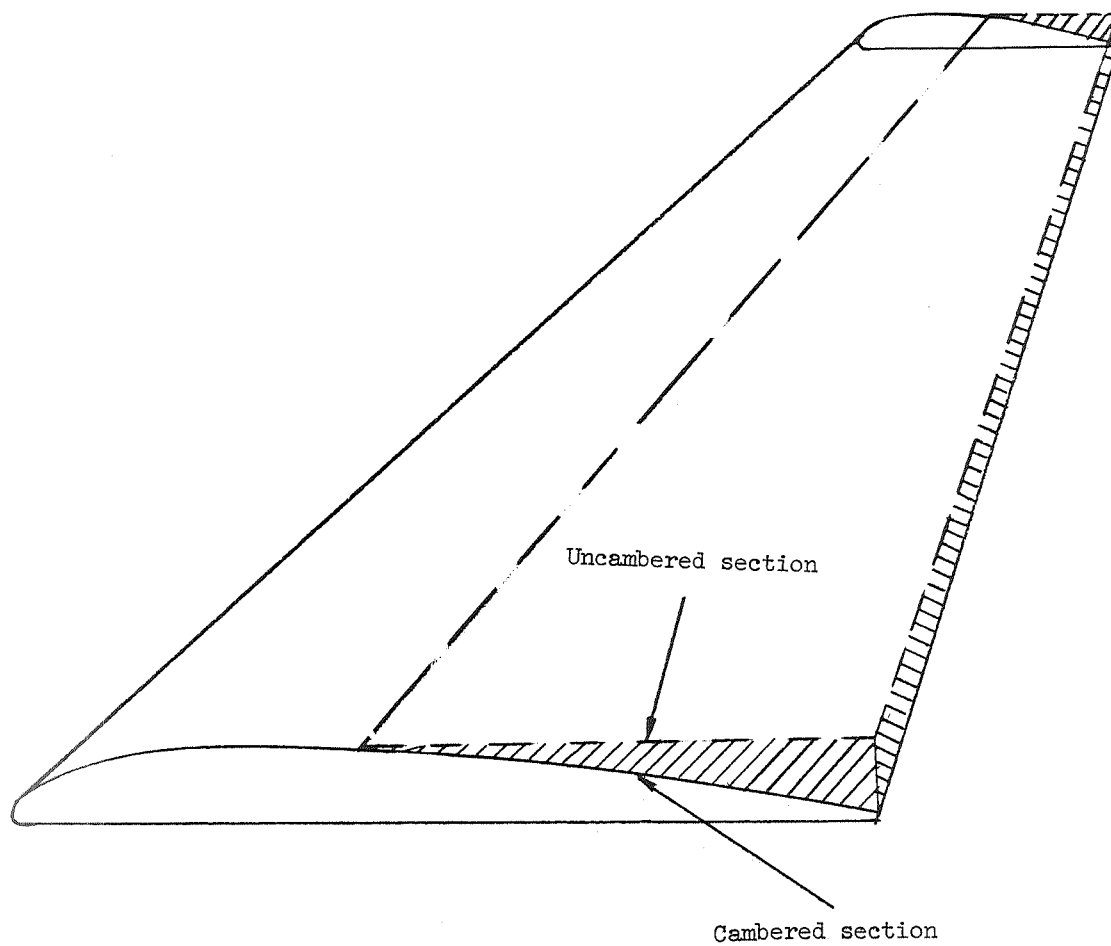
Top and side views



Body cross-section station, $x/l = 1.00$

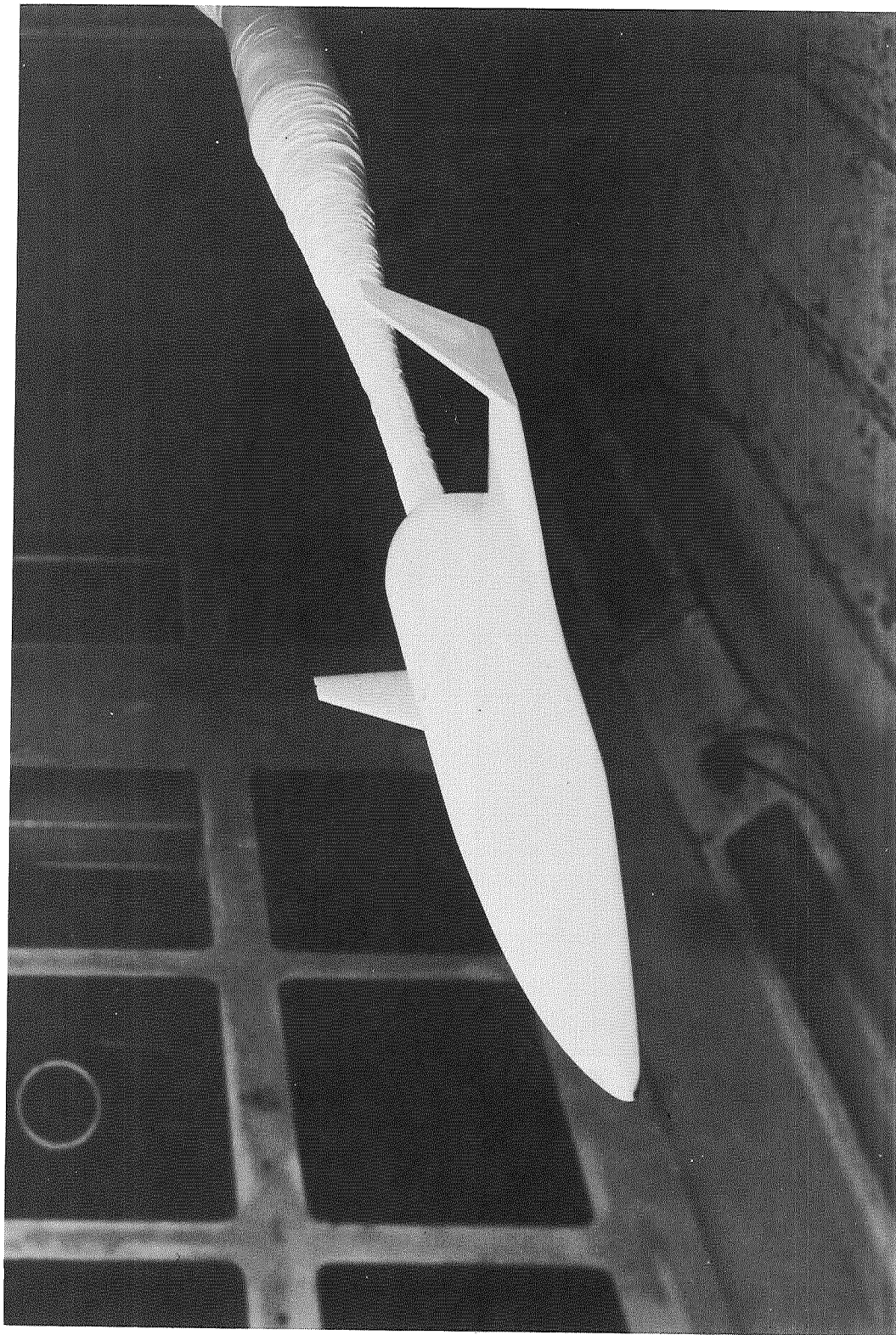
(c) Body boattailing details.

Figure 2.- Continued.



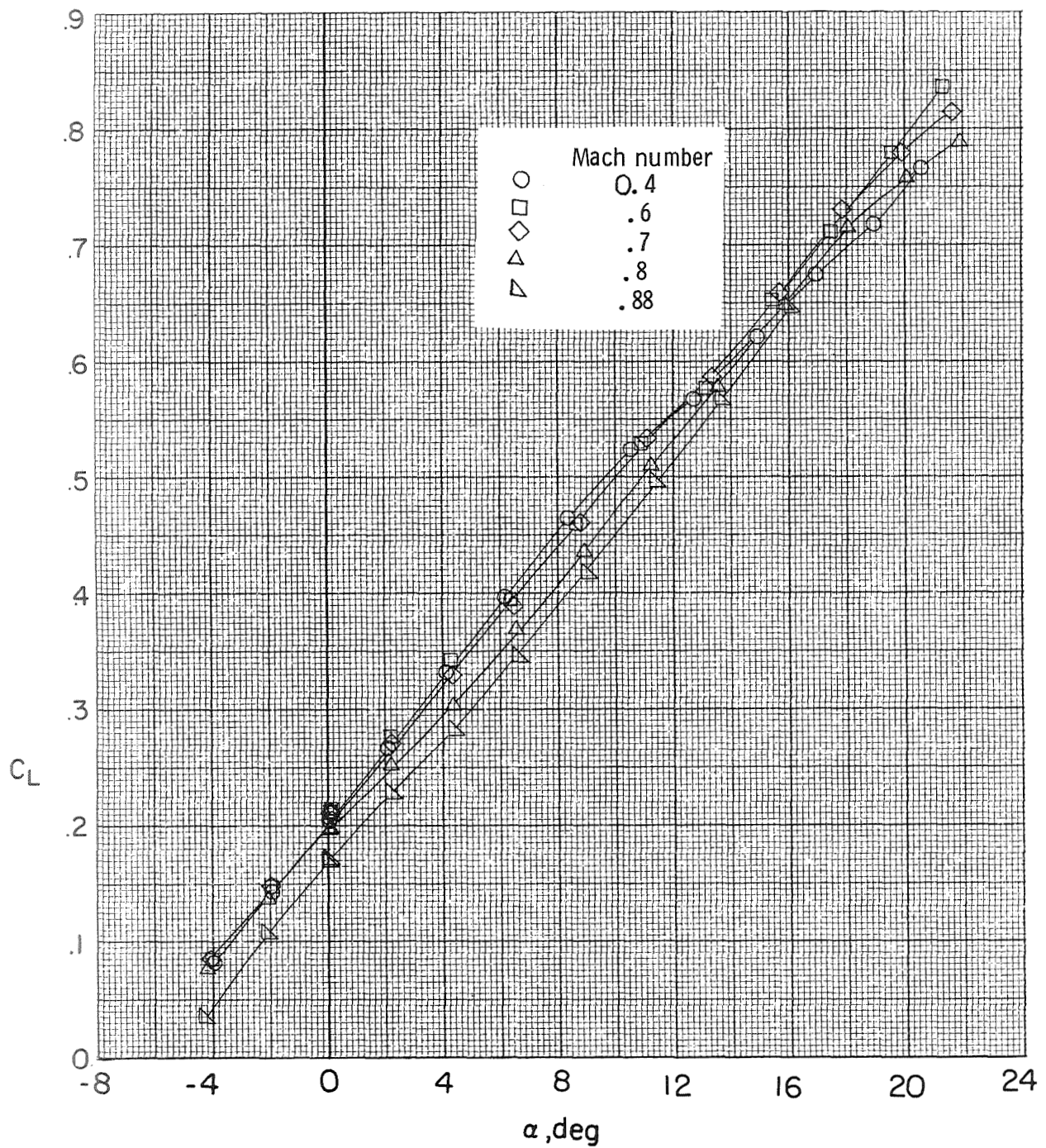
(d) Vertical-tail cross sections.

Figure 2.- Concluded.



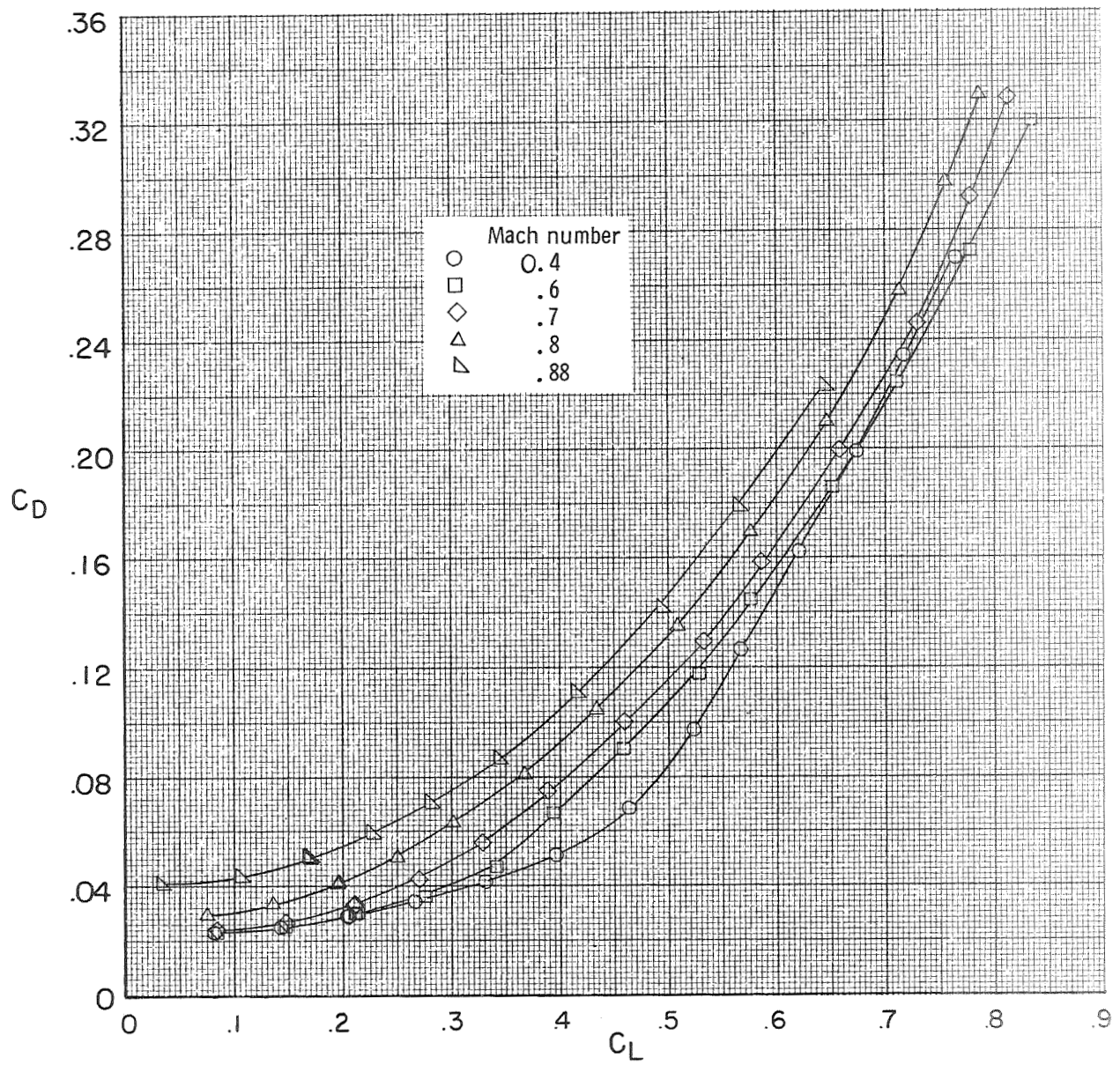
L-70-5593

Figure 3.- Photograph of model mounted for tests in the Langley high-speed 7- by 10-foot tunnel.



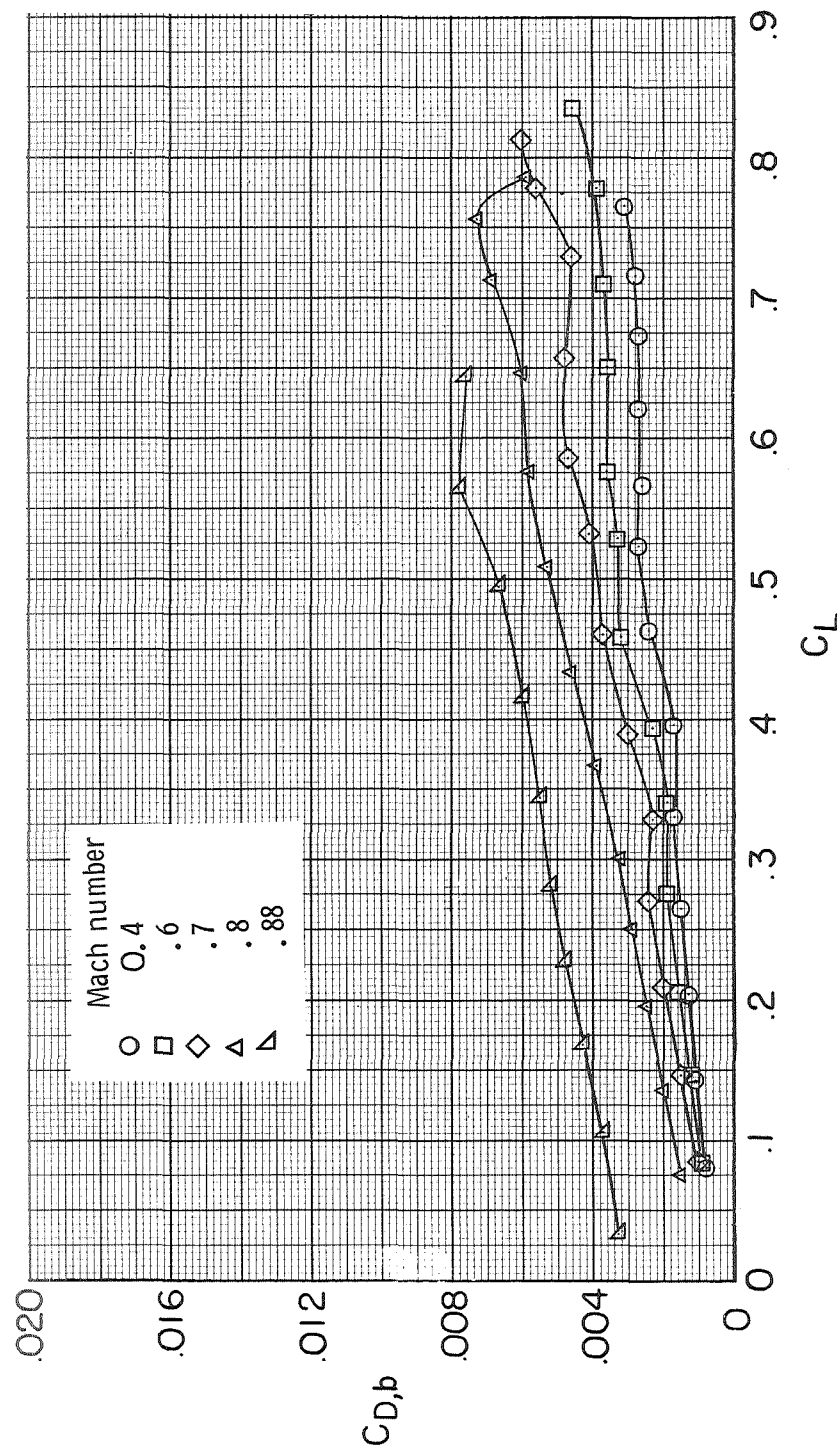
(a) C_L as a function of α .

Figure 4.- Effect of Mach number on longitudinal aerodynamic characteristics of model. $\delta_e = 0^\circ$.



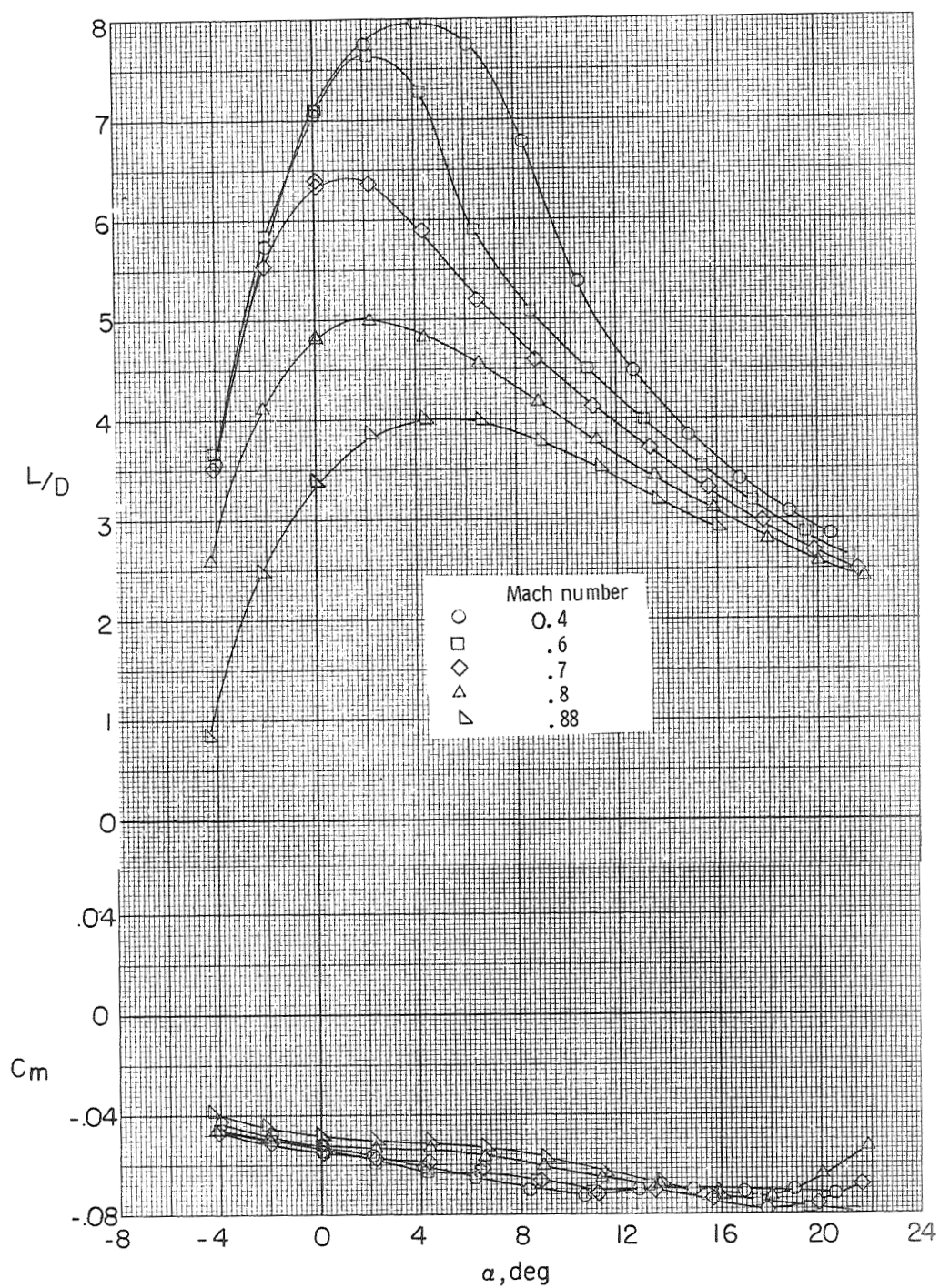
(b) C_D as a function of C_L .

Figure 4.- Continued.



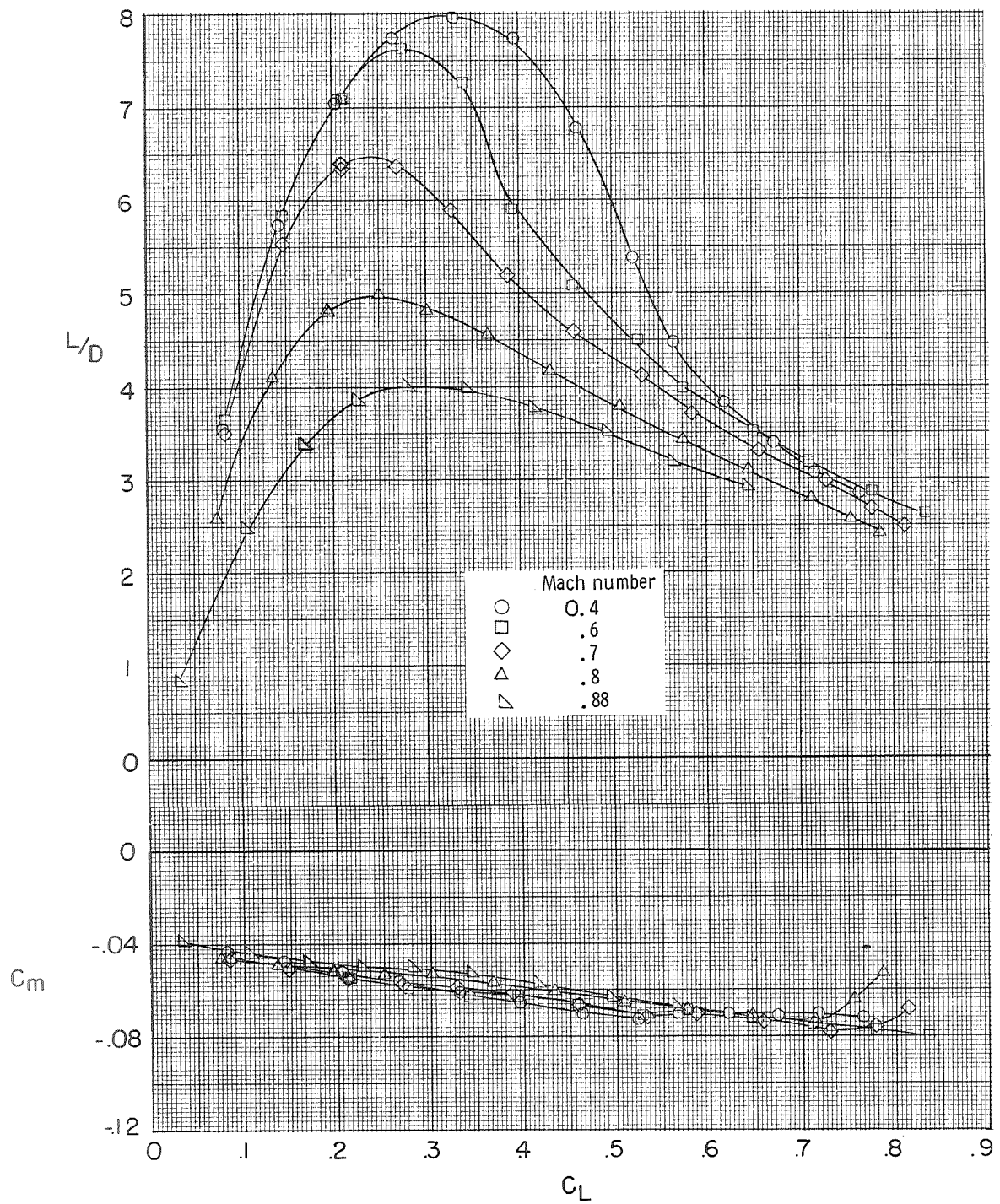
(c) Base-drag coefficient.

Figure 4.- Continued.



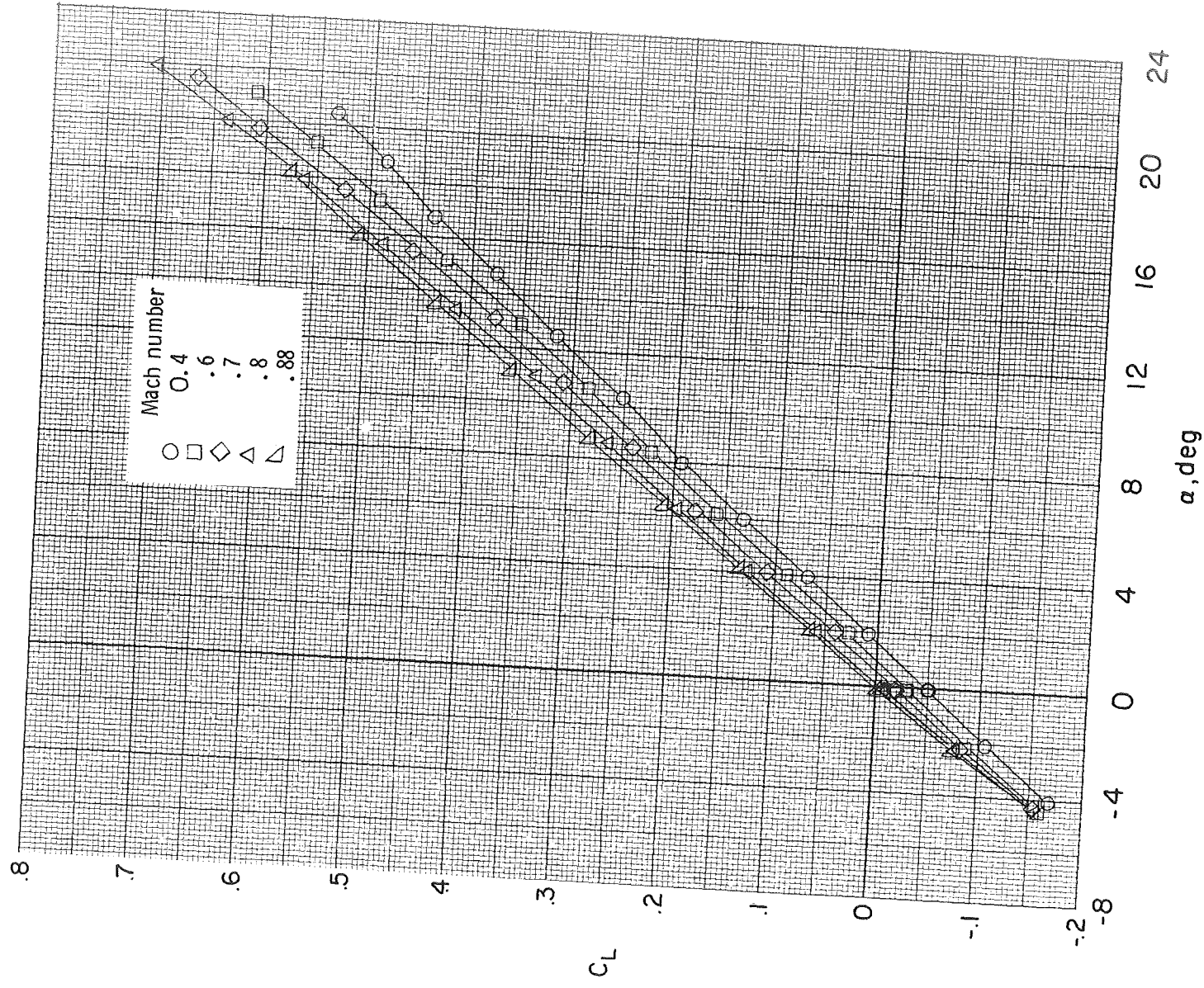
(d) C_m and L/D as functions of α .

Figure 4.- Continued.

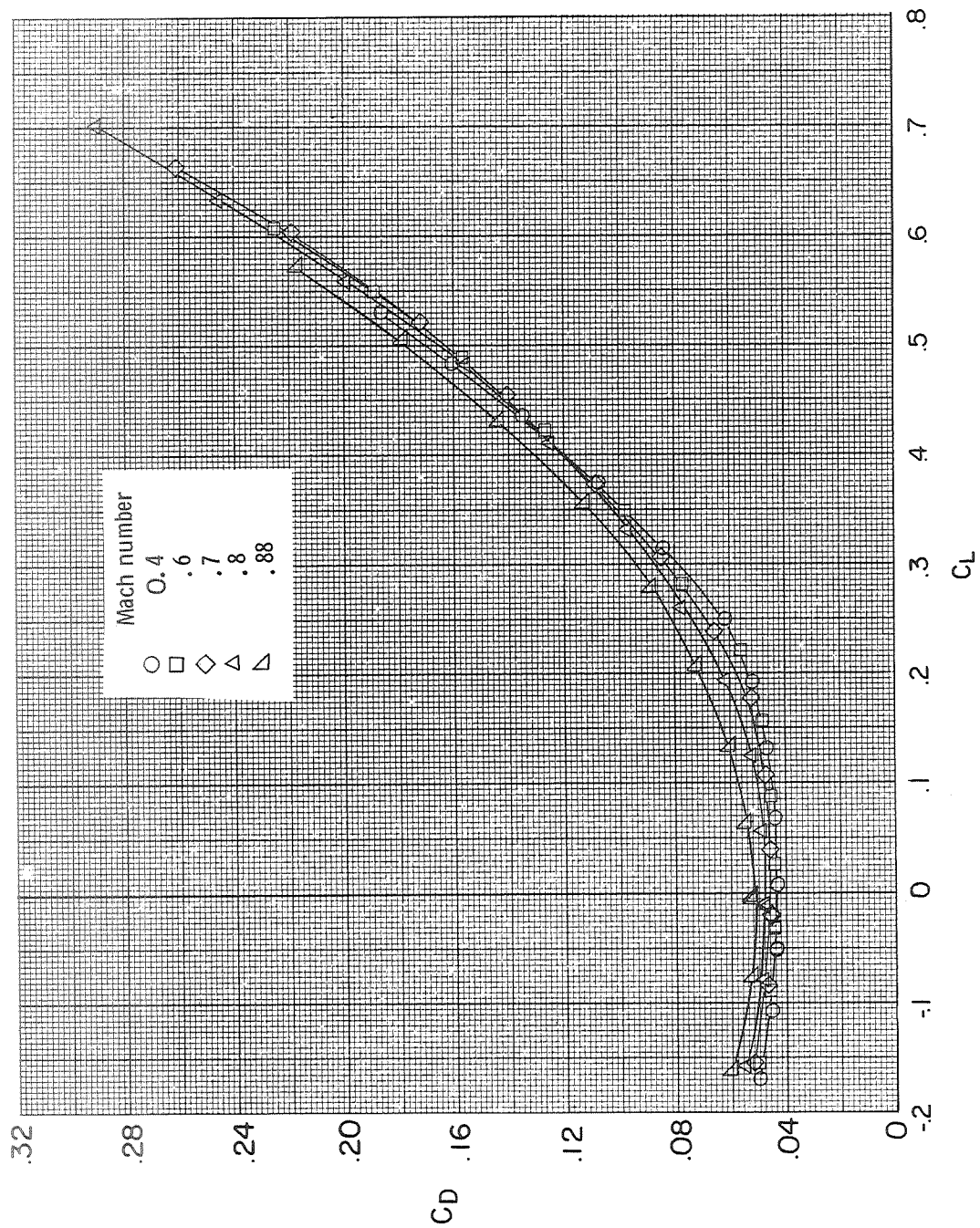


(e) C_m and L/D as functions of C_L .

Figure 4.- Concluded.

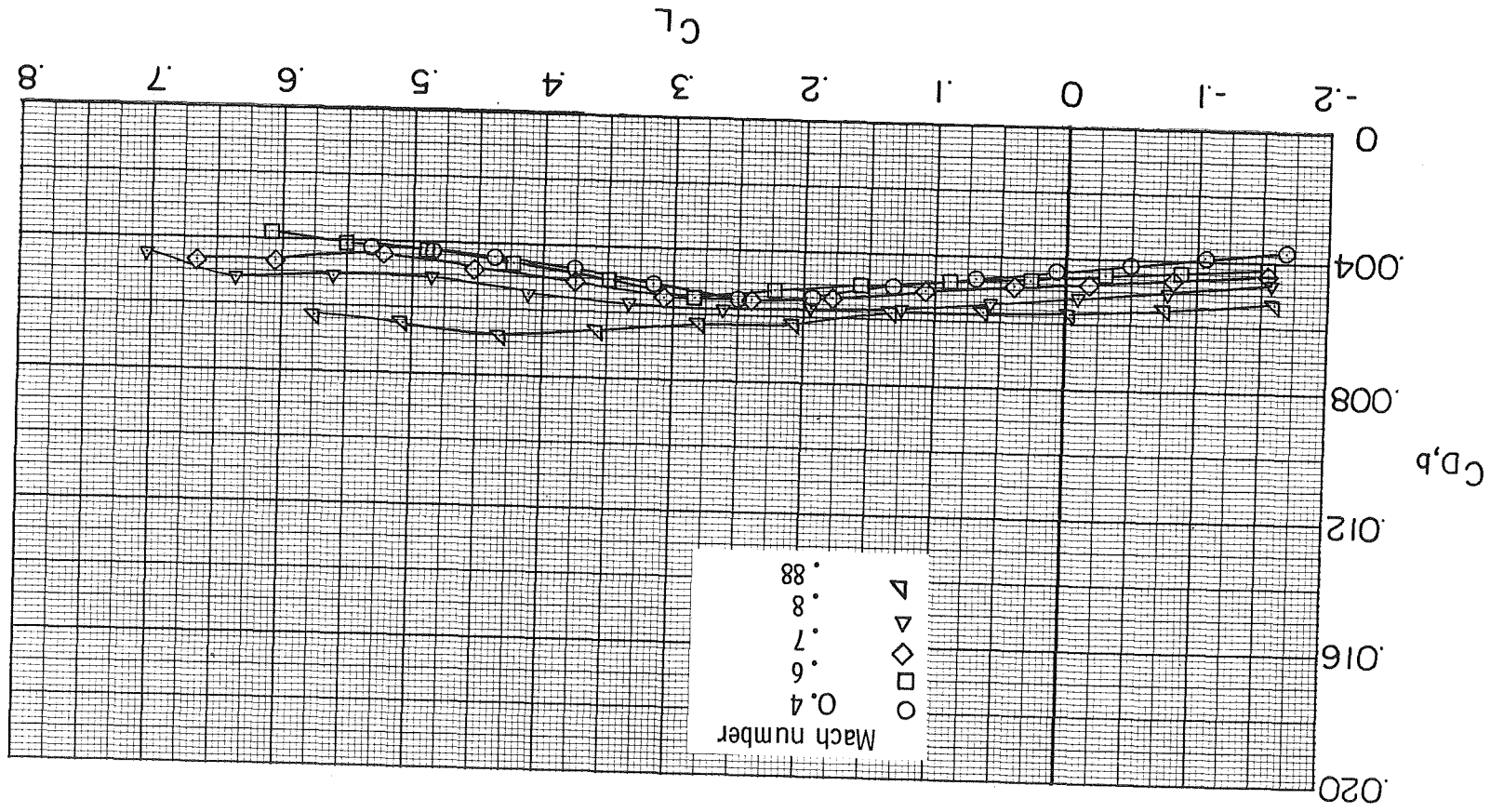


(a) C_L as a function of α .
 Figure 5.- Effect of Mach number on longitudinal aerodynamic characteristics
 of model. $\delta_e = -30^\circ$.

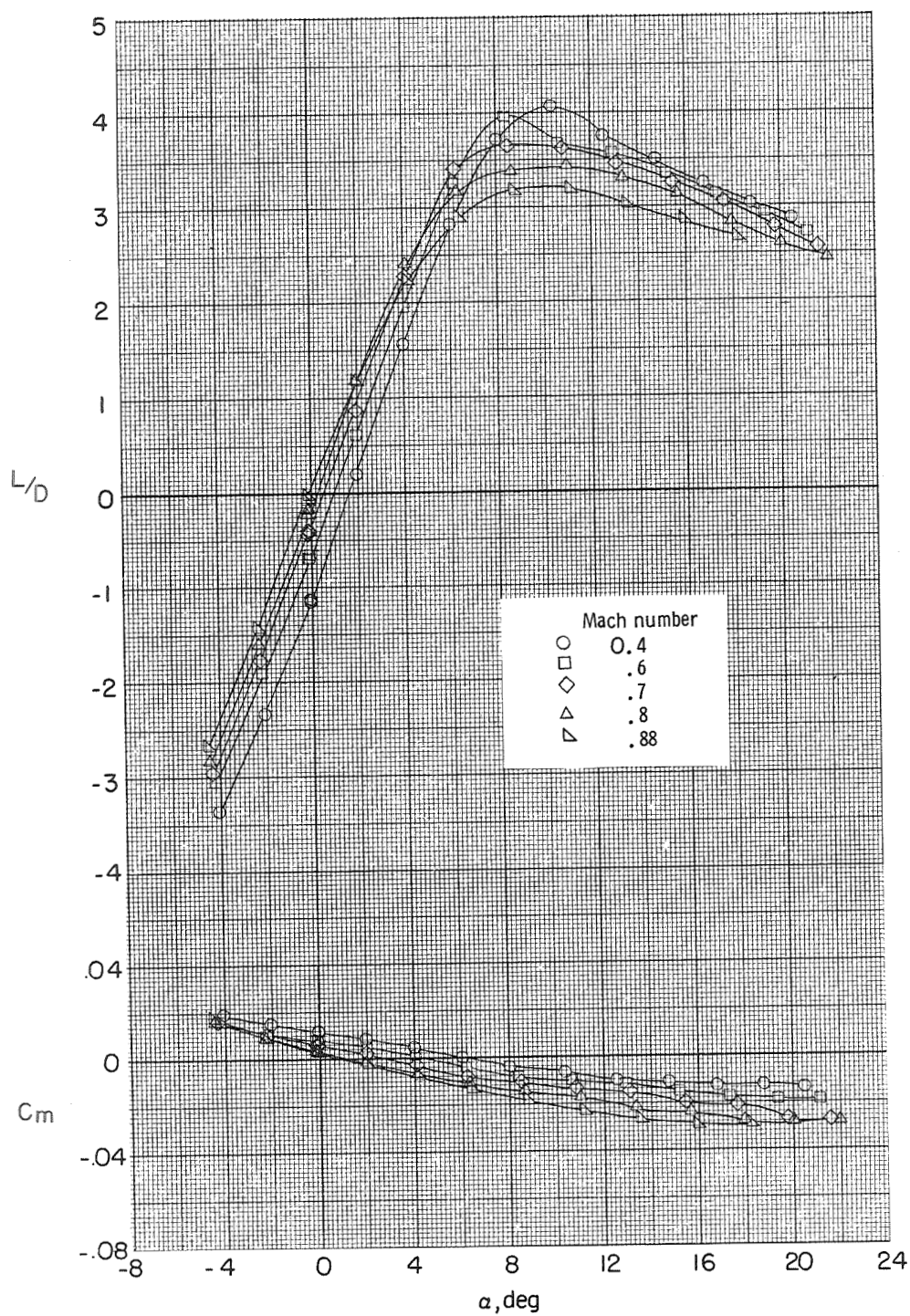


(b) C_D as a function of C_L .

Figure 5.- Continued.

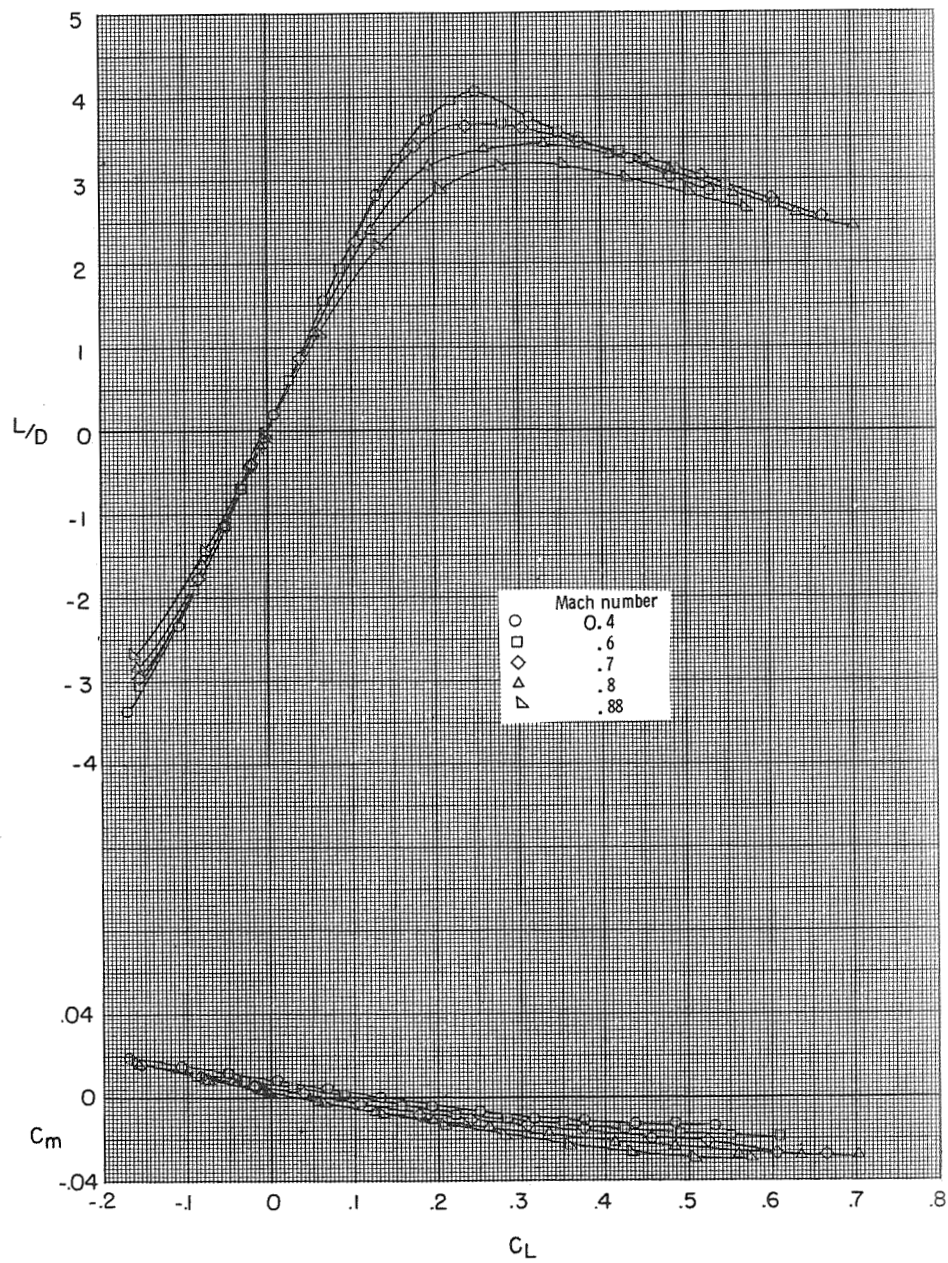


(c) Base-drag coefficient.
Figure 5.- Continued.



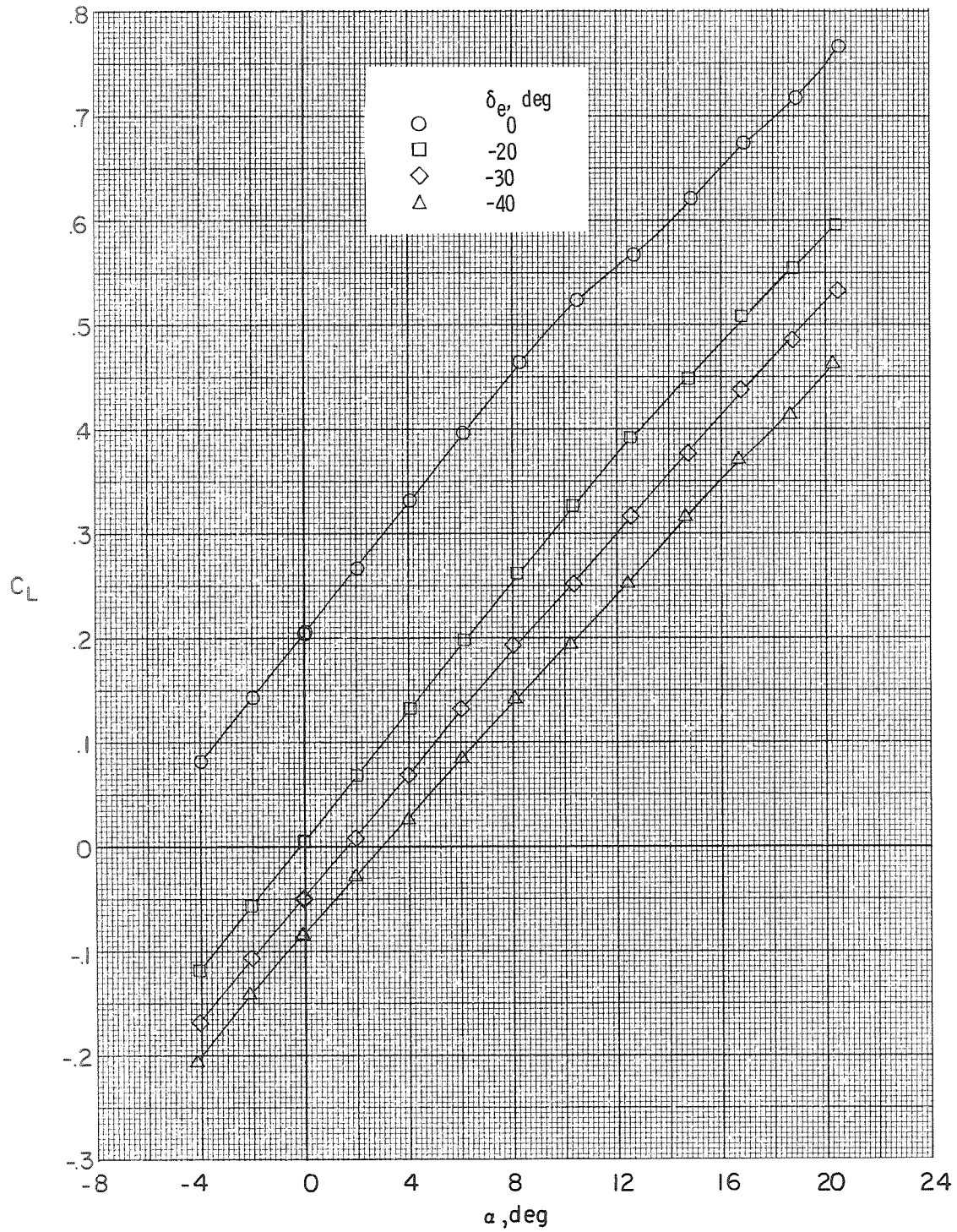
(d) C_m and L/D as functions of α .

Figure 5.- Continued.



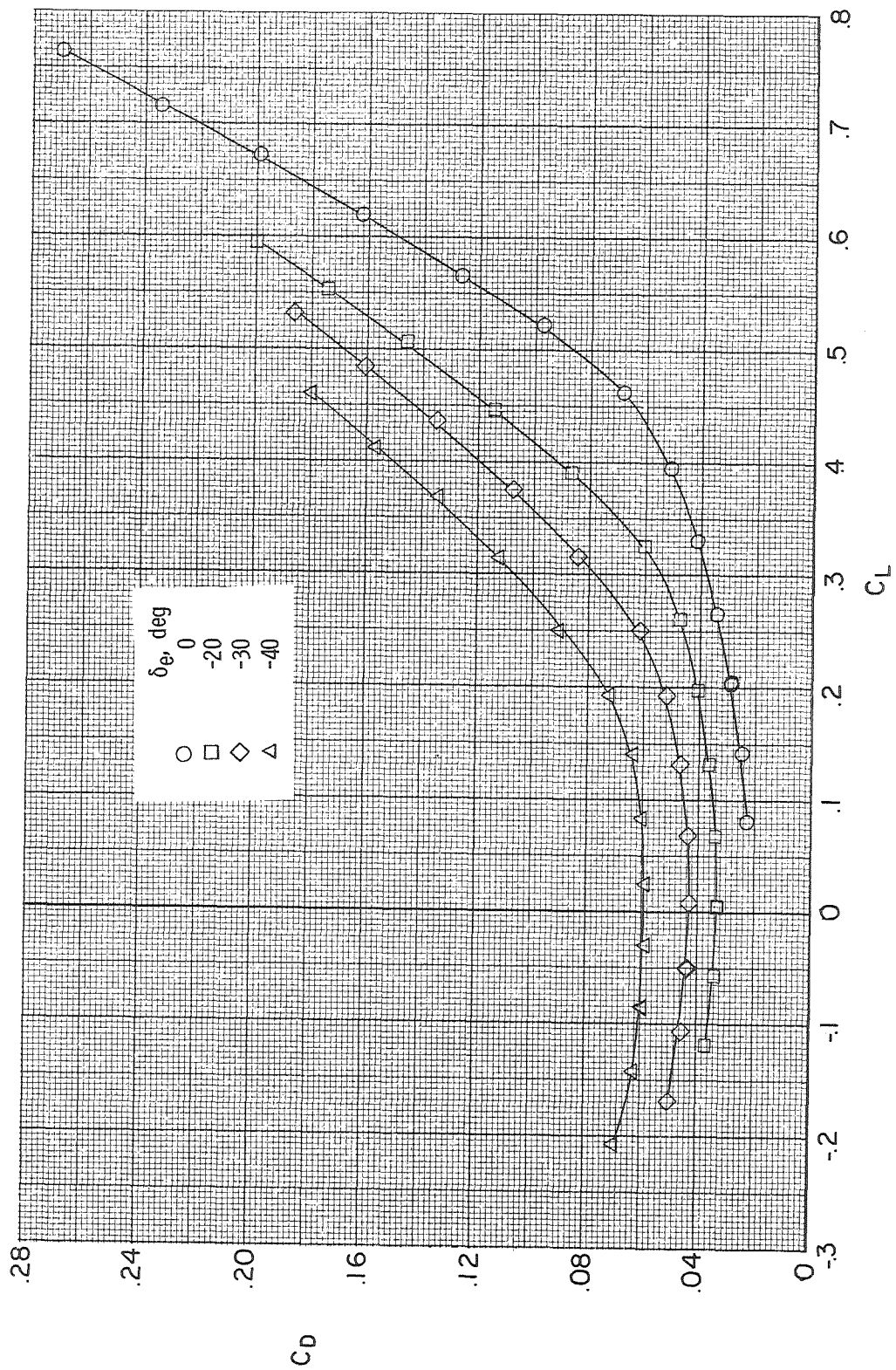
(e) C_m and L/D as functions of C_L .

Figure 5.- Concluded.



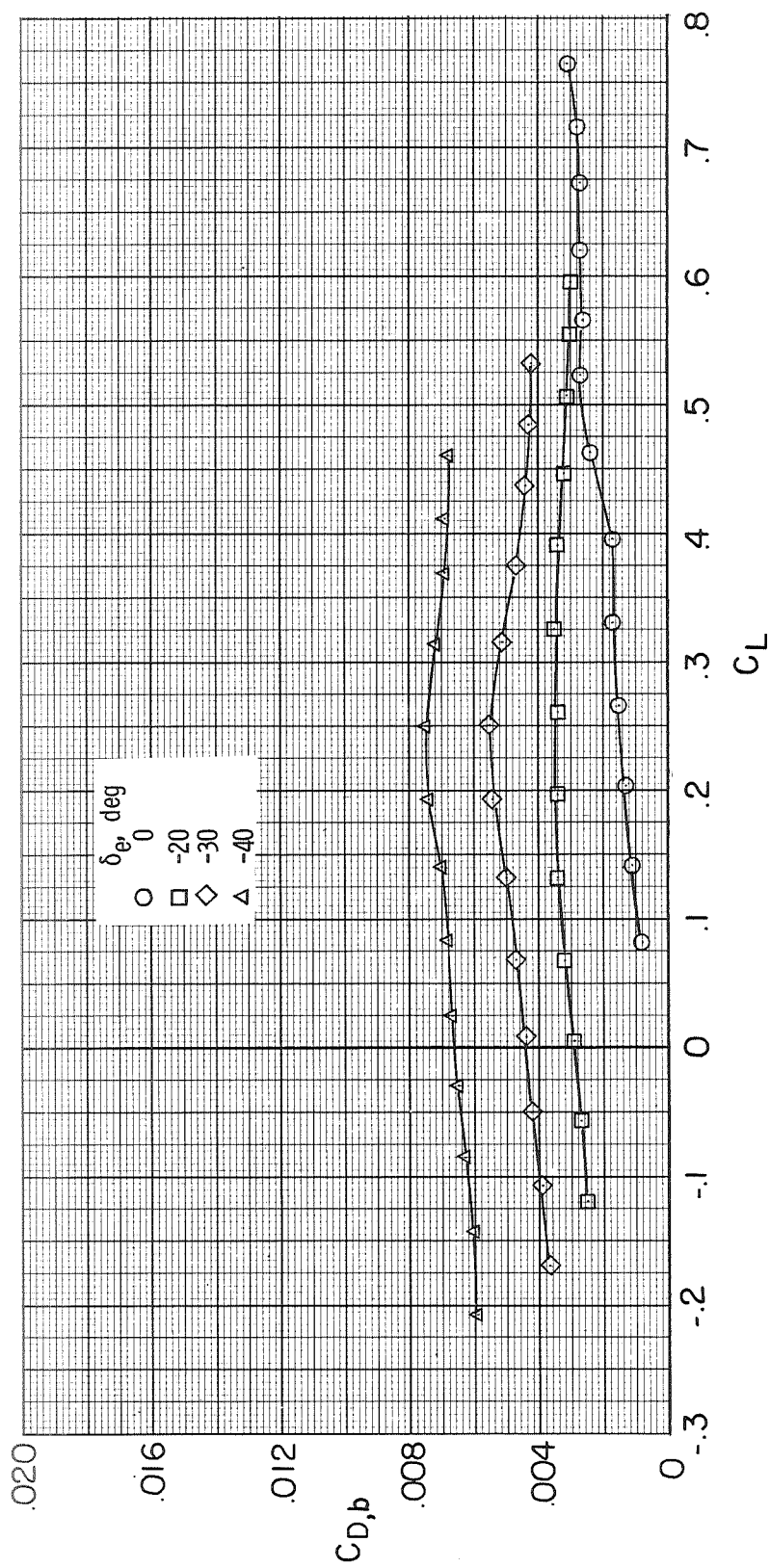
(a) C_L as a function of α .

Figure 6.- Longitudinal-control effectiveness. $M = 0.4$.



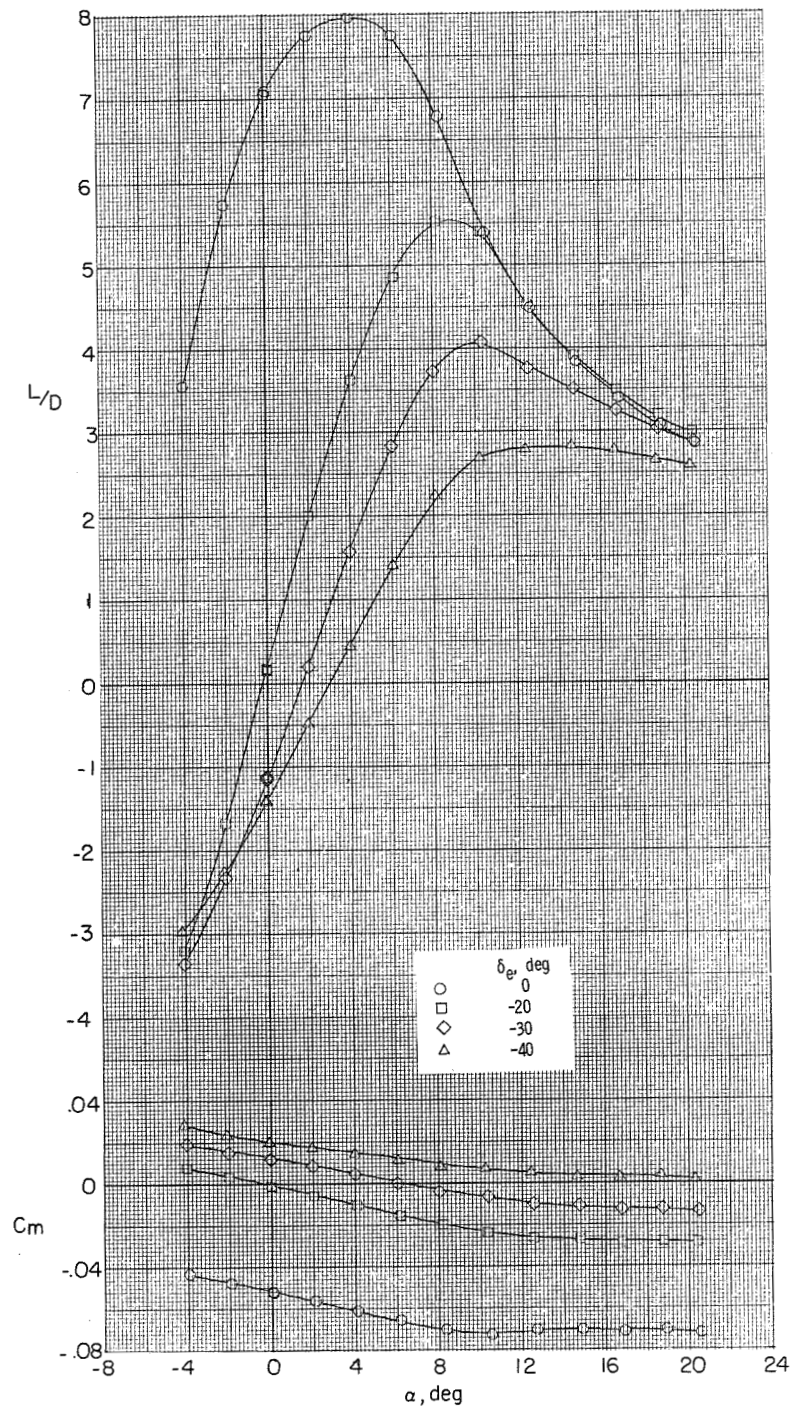
(b) C_D as a function of C_L .

Figure 6.- Continued.



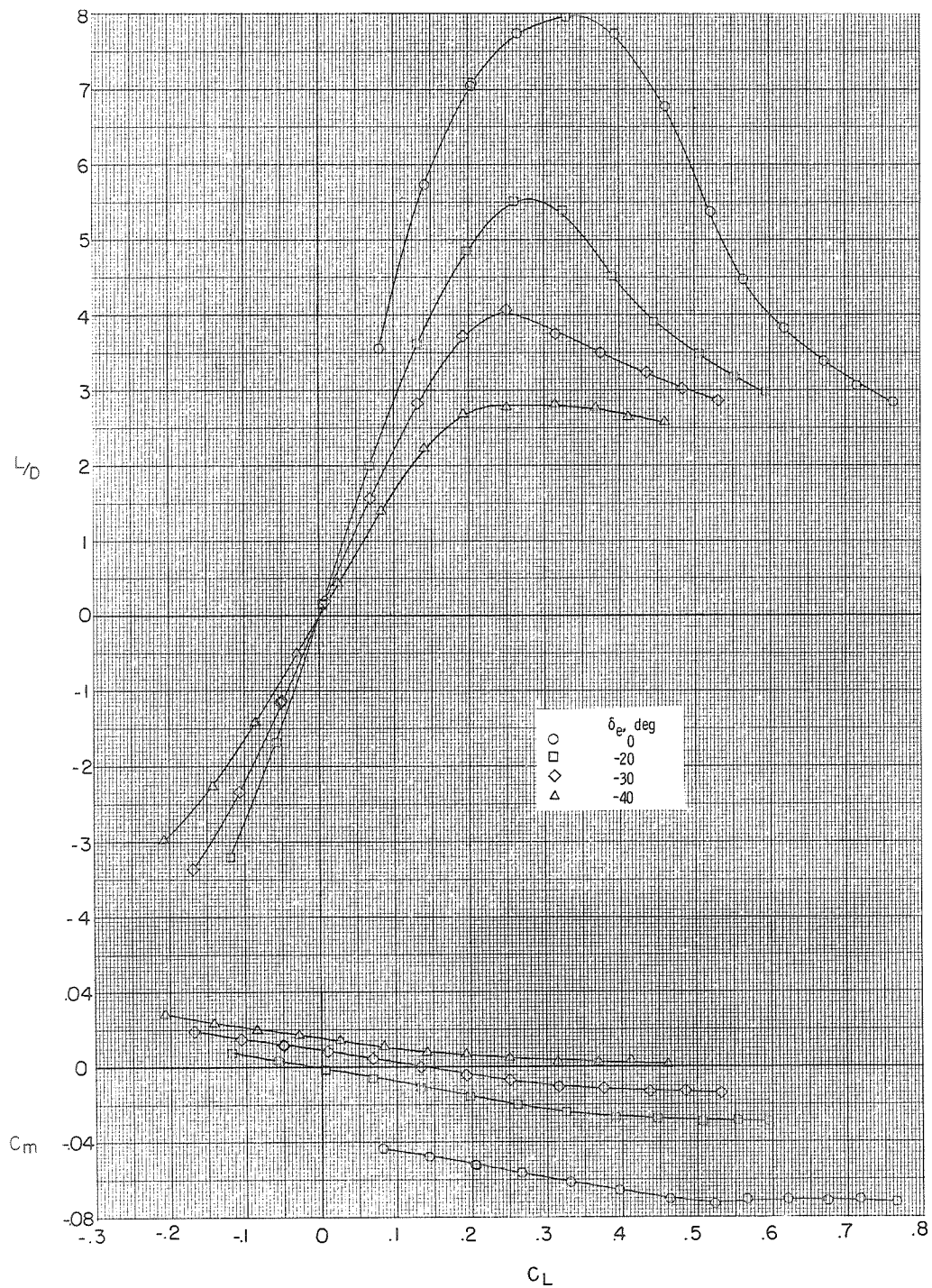
(c) Base-drag coefficient.

Figure 6.- Continued.



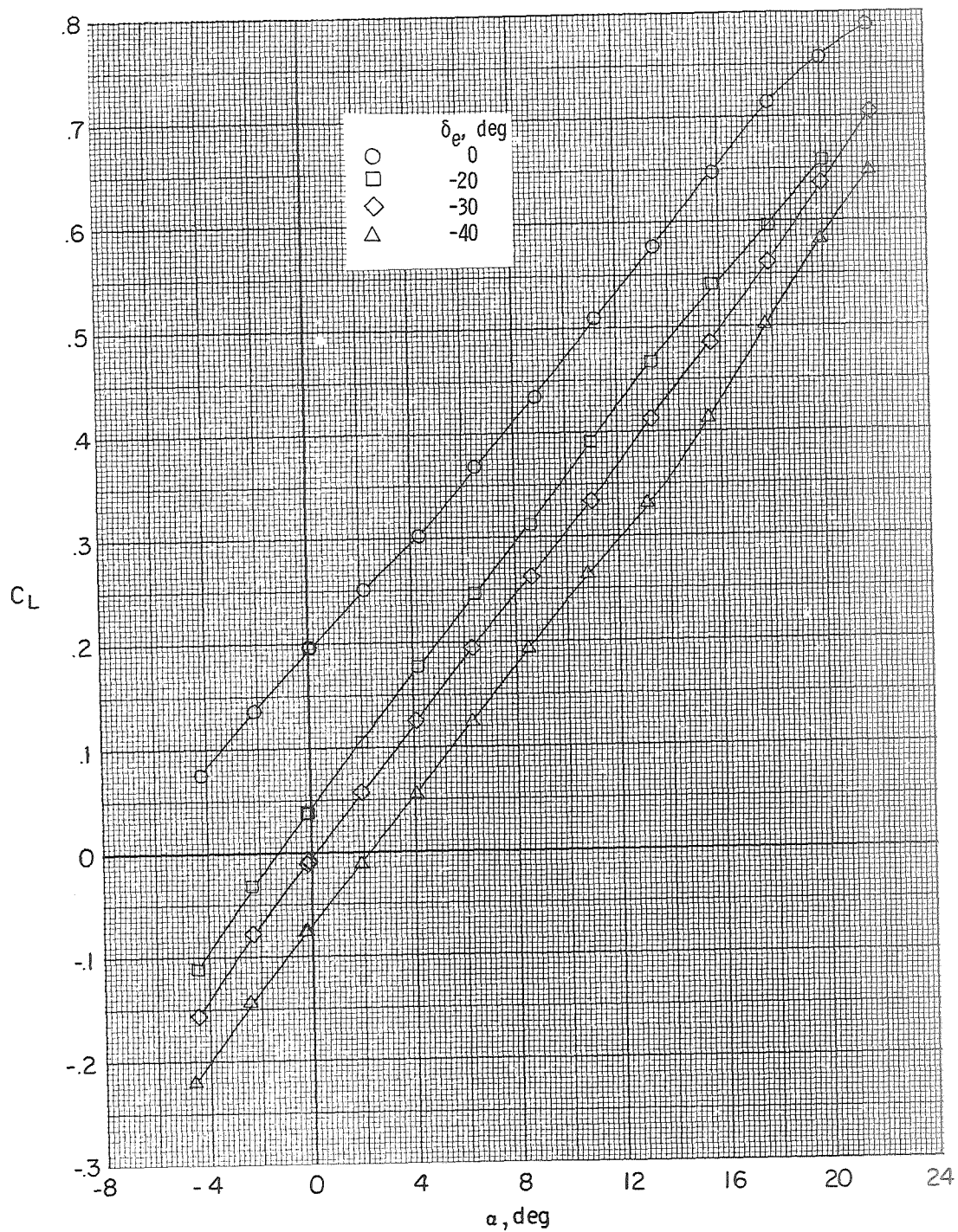
(d) C_m and L/D as functions of α .

Figure 6.- Continued.



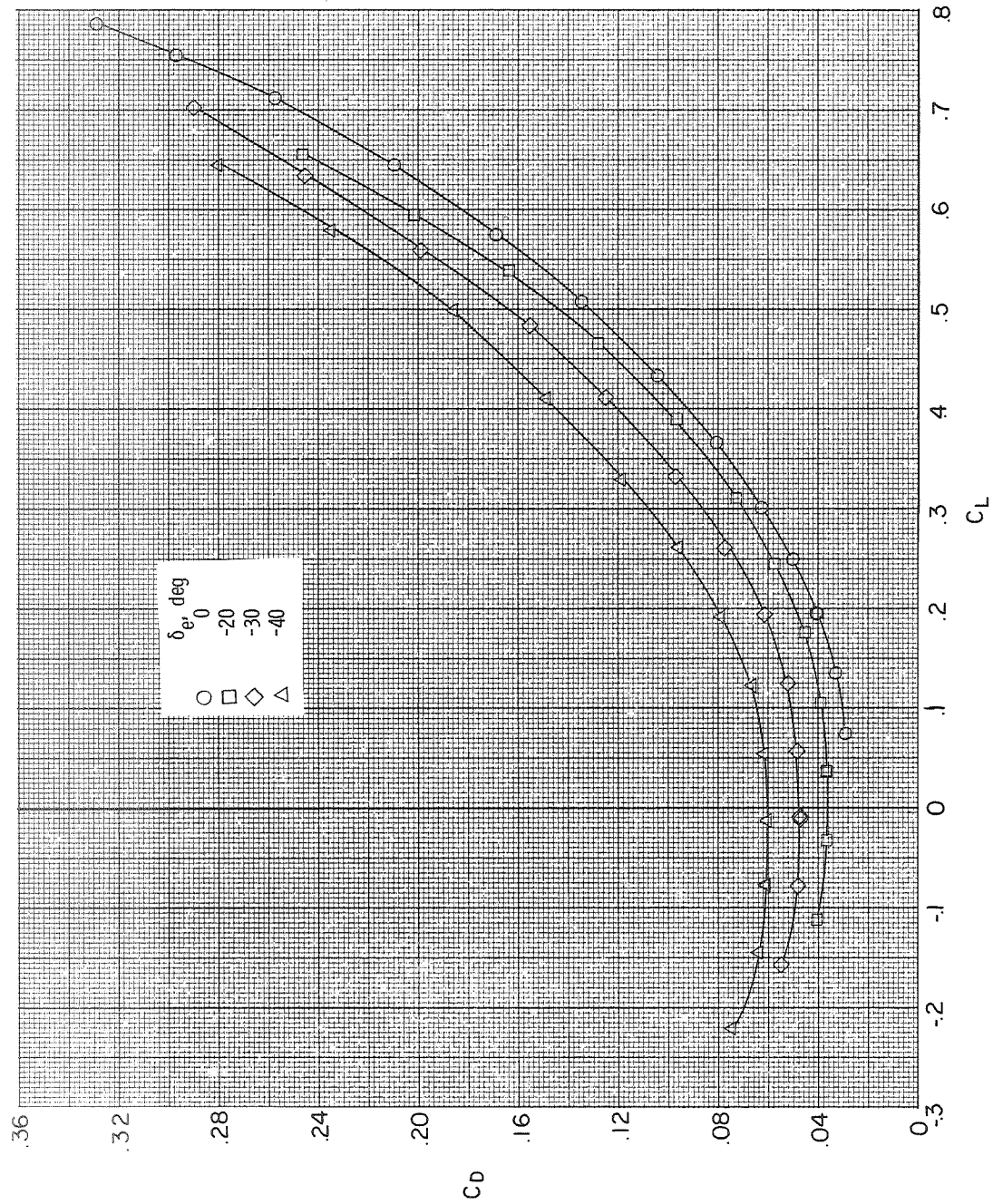
(e) C_m and L/D as functions of C_L .

Figure 6.- Concluded.



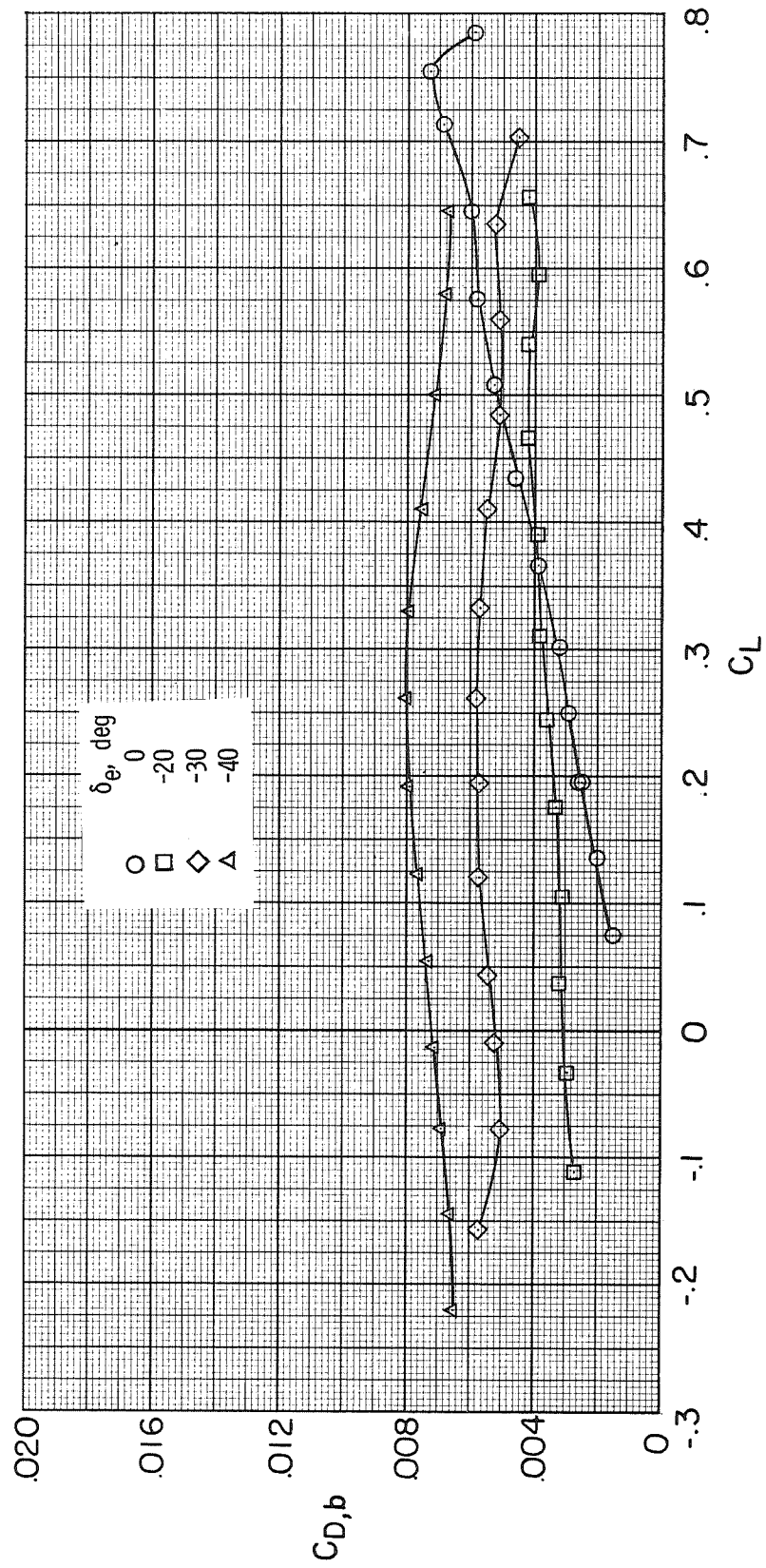
(a) C_L as a function of α .

Figure 7.- Longitudinal-control effectiveness. $M = 0.8$.



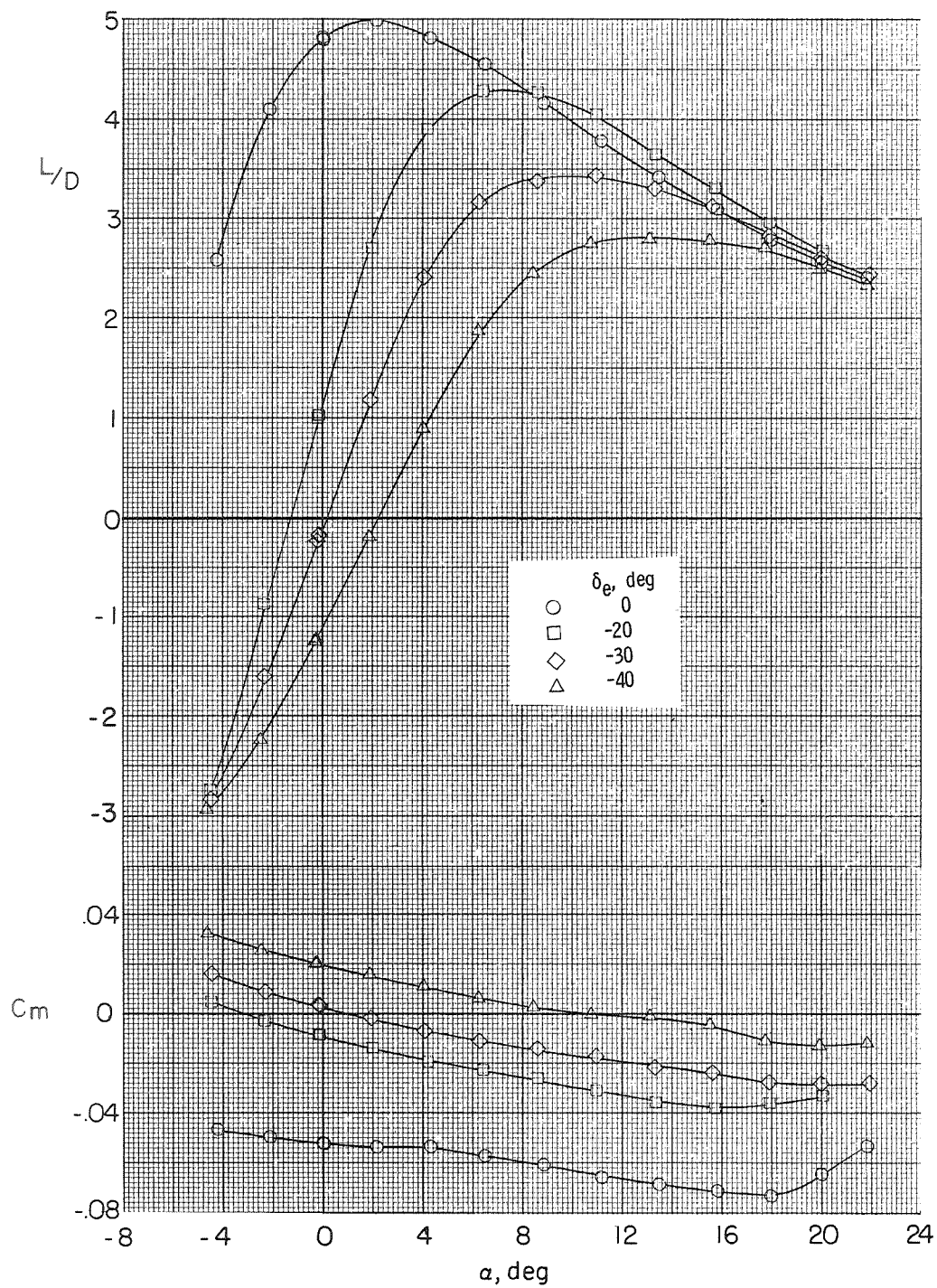
(b) C_D as a function of C_L .

Figure 7.- Continued.



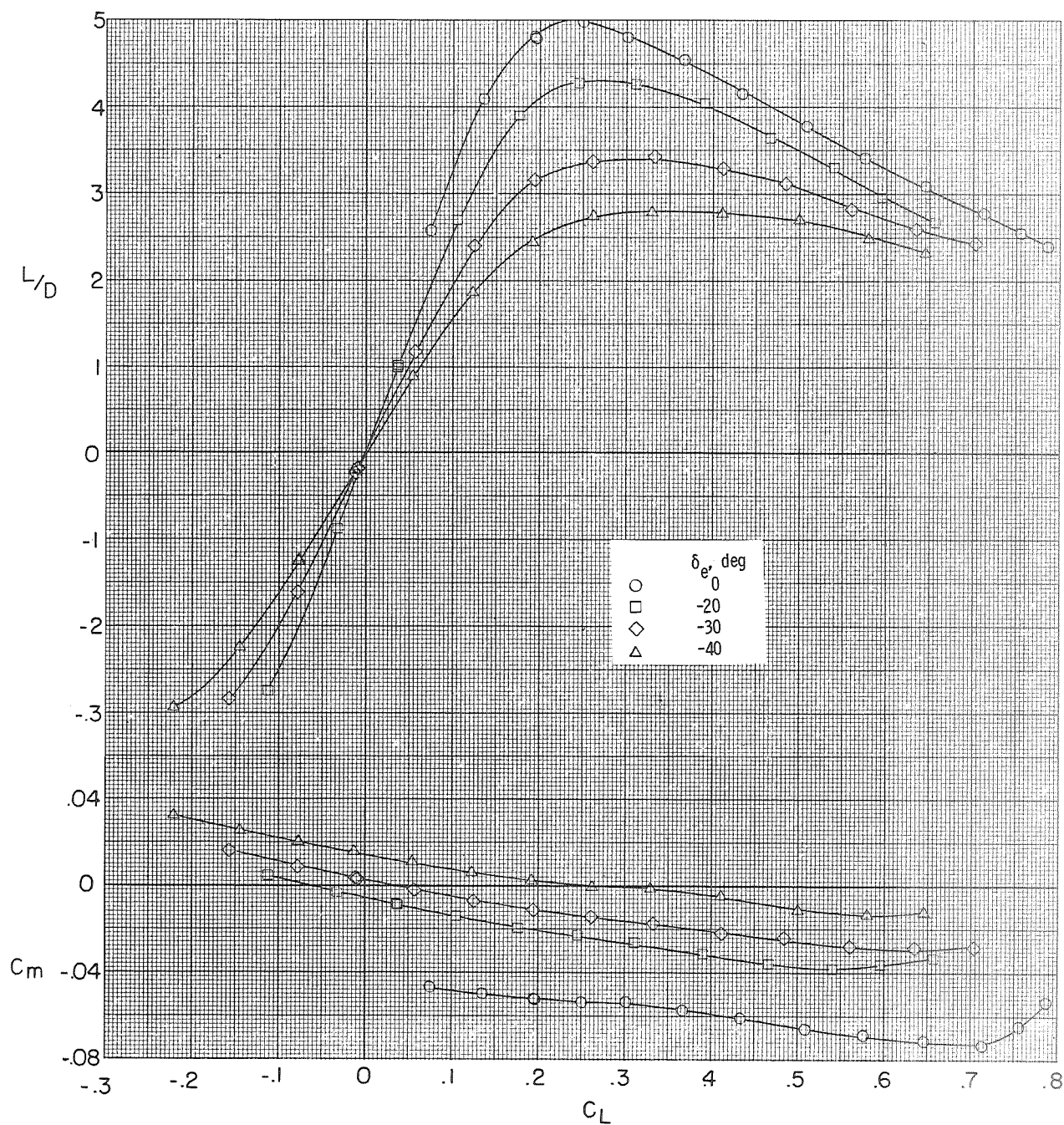
(c) Base-drag coefficient.

Figure 7.- Continued.



(d) C_m and L/D as functions of α .

Figure 7.- Continued.



(e) C_m and L/D as functions of C_L .

Figure 7.- Concluded.

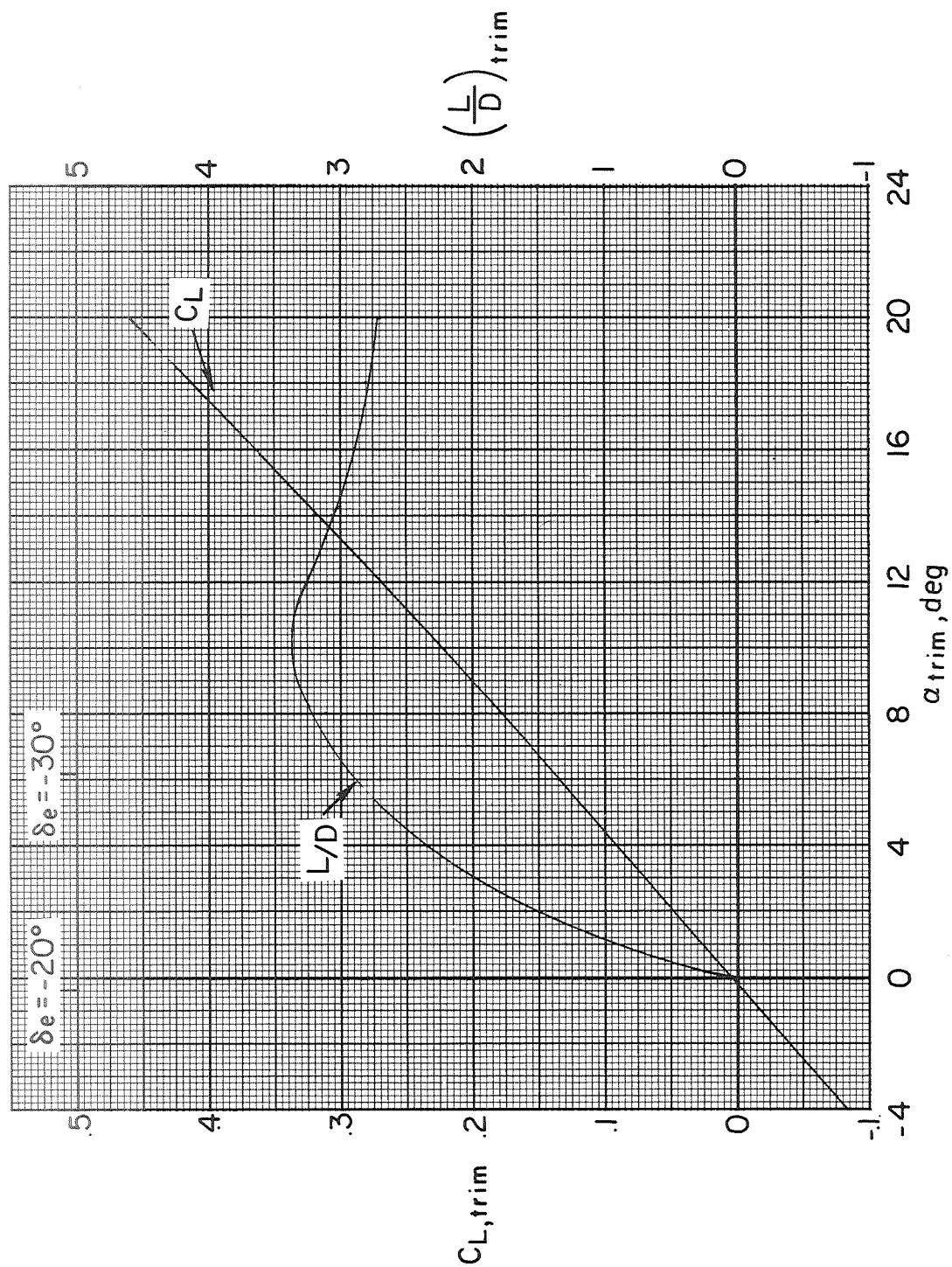
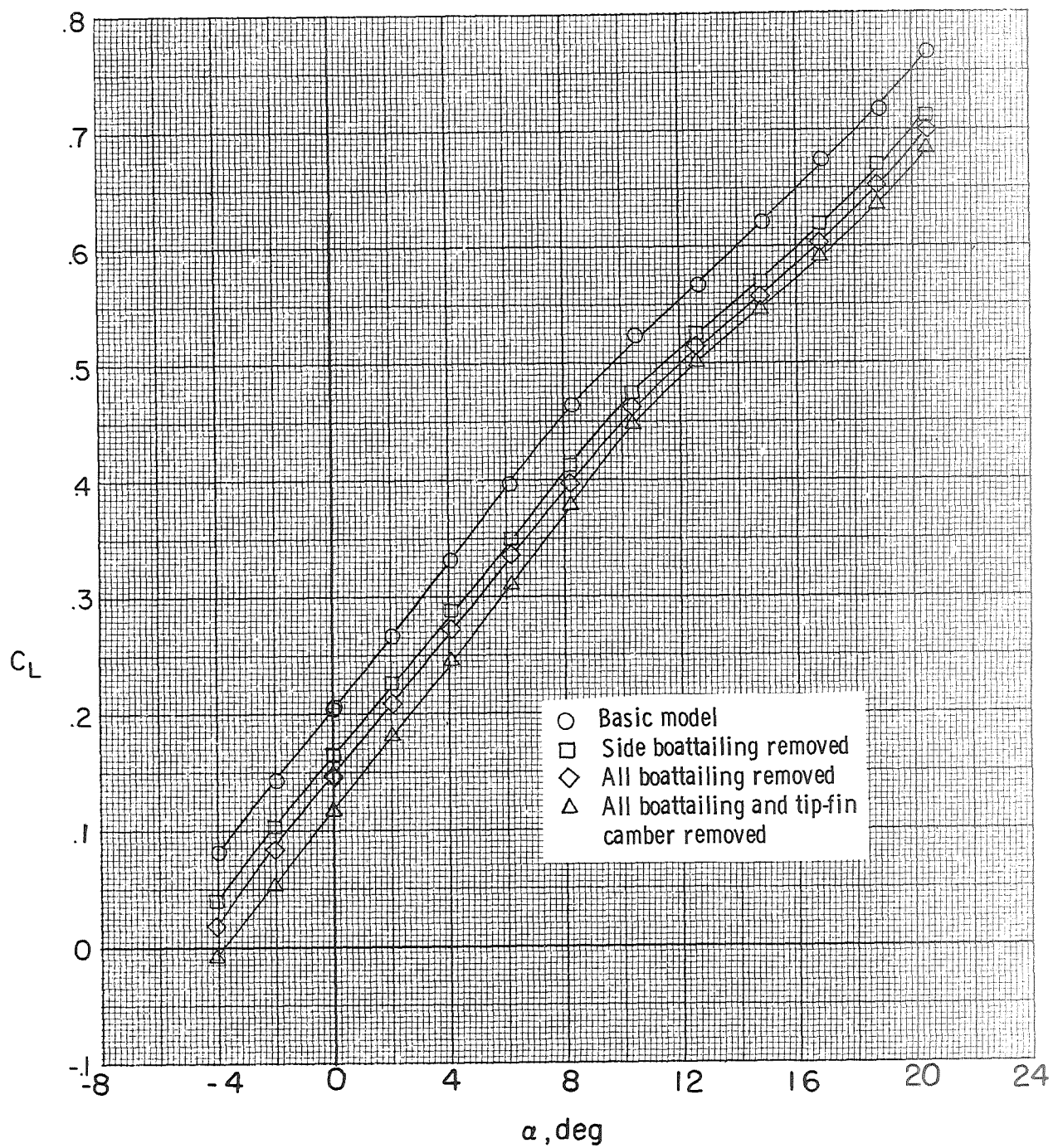
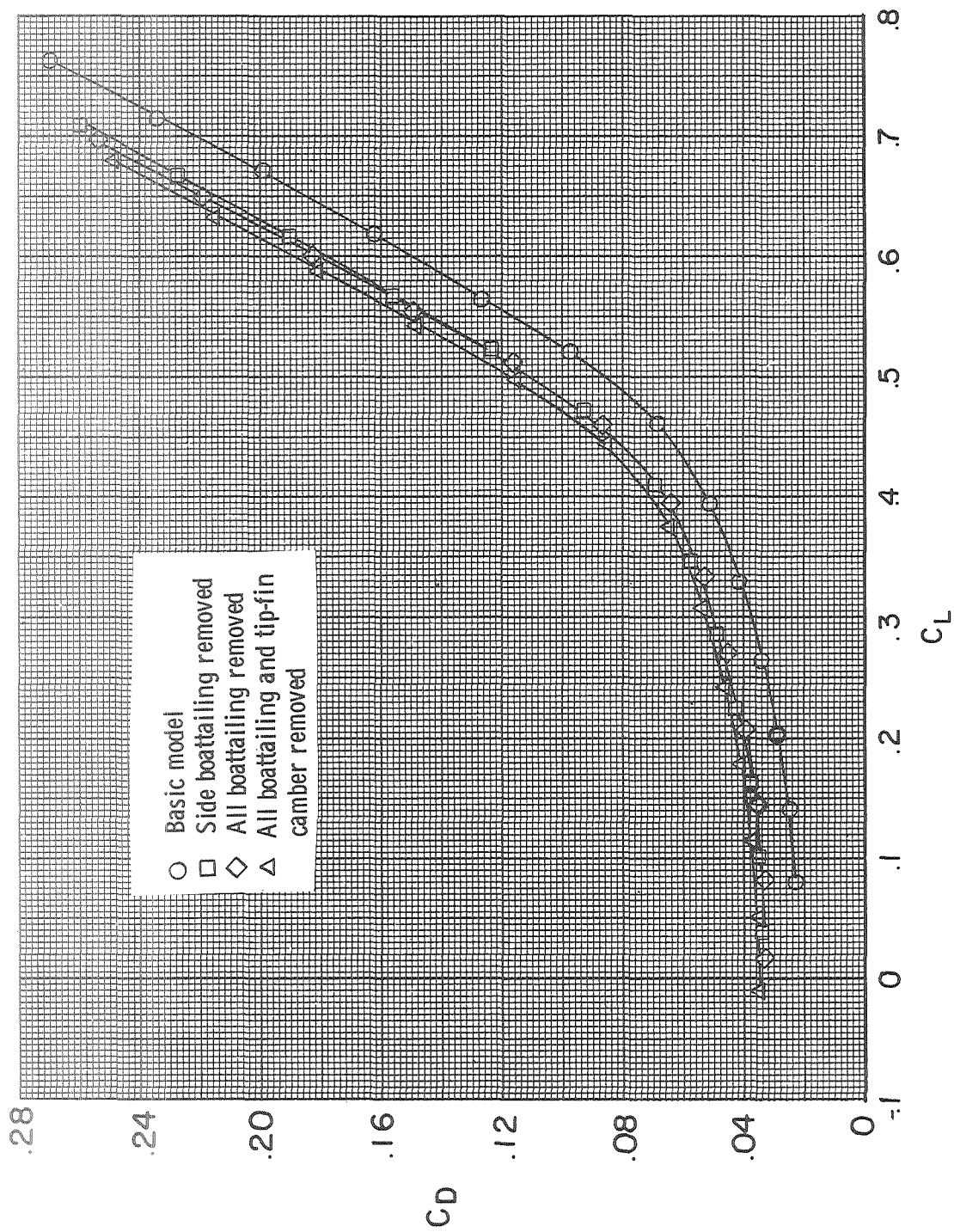


Figure 8.- Trim-performance characteristics of the basic model. $M = 0.4$.



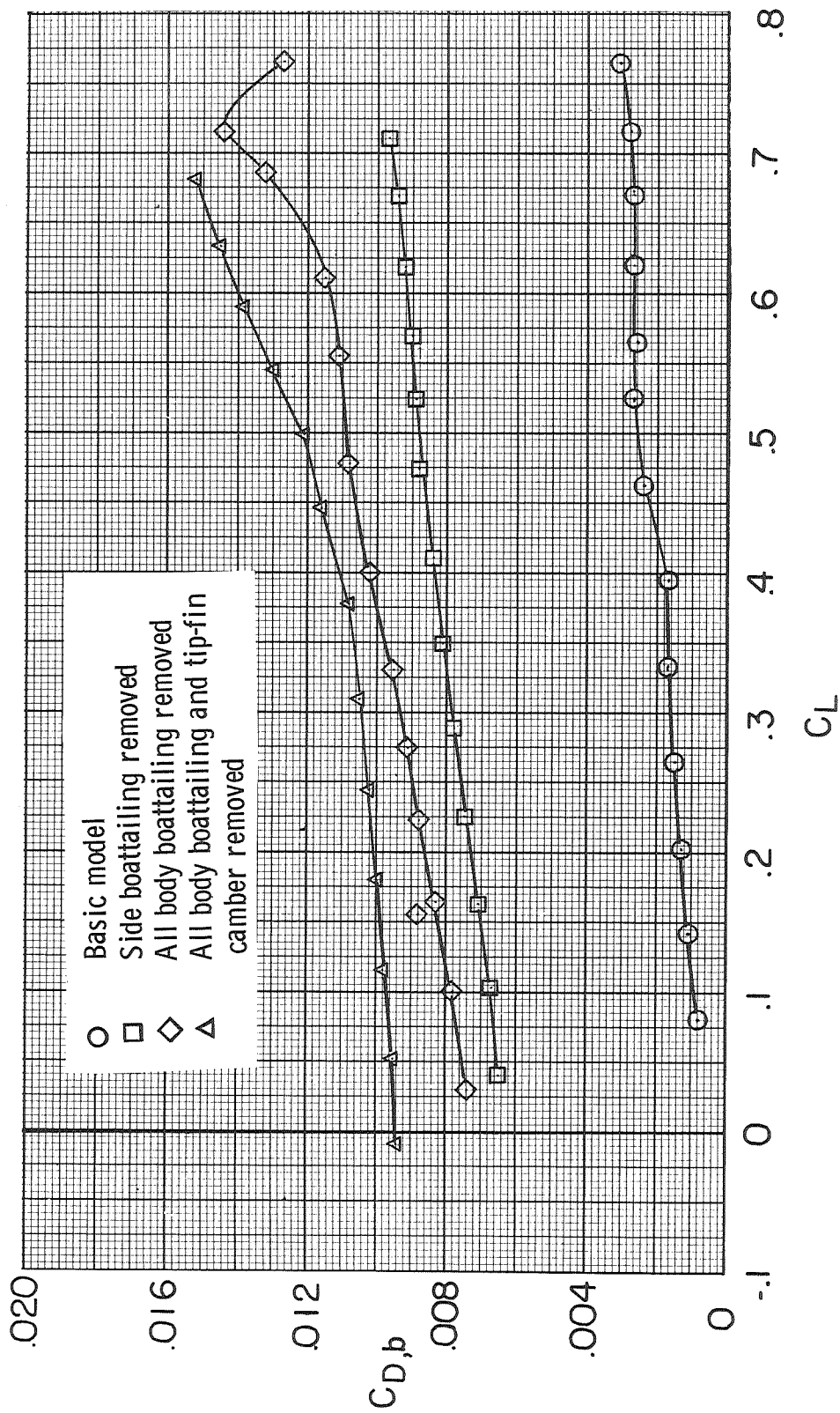
(a) C_L as a function of α .

Figure 9.- Effect of afterbody and tip-fin modifications on longitudinal aerodynamic characteristics of model. $\delta_e = 0^\circ$; $M = 0.4$.



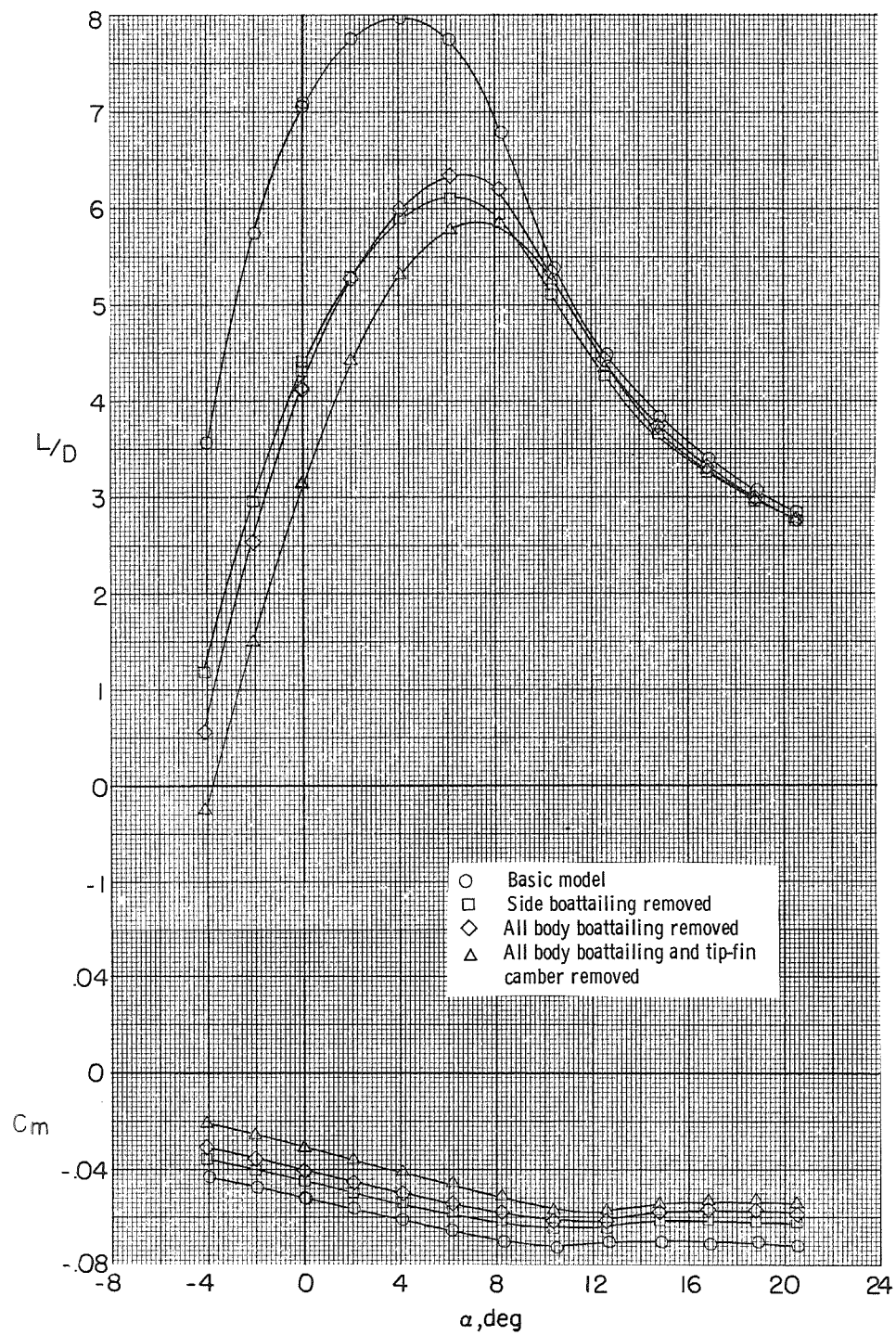
(b) C_D as a function of C_L .

Figure 9.- Continued.



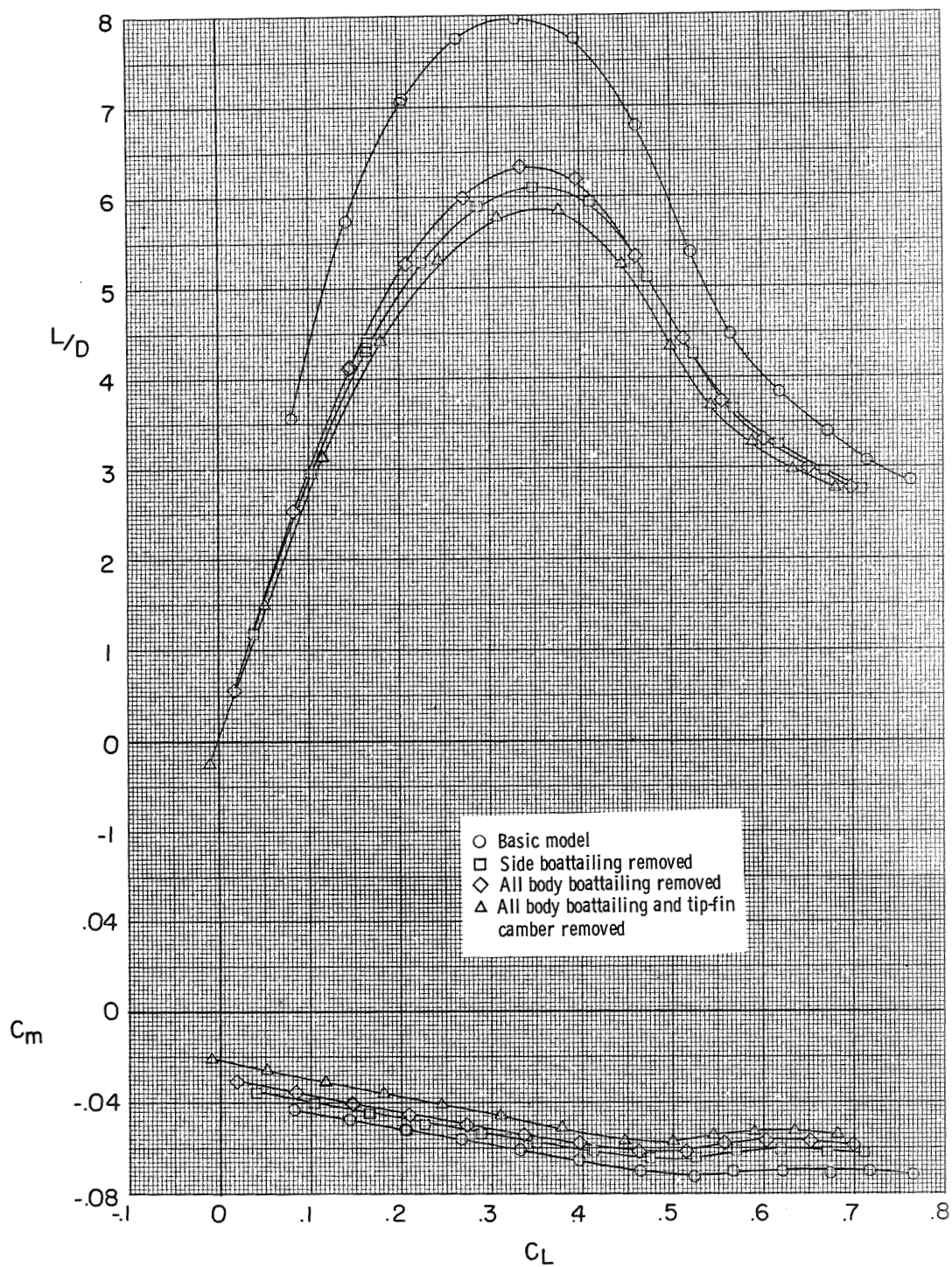
(c) Base-drag coefficient.

Figure 9.- Continued.



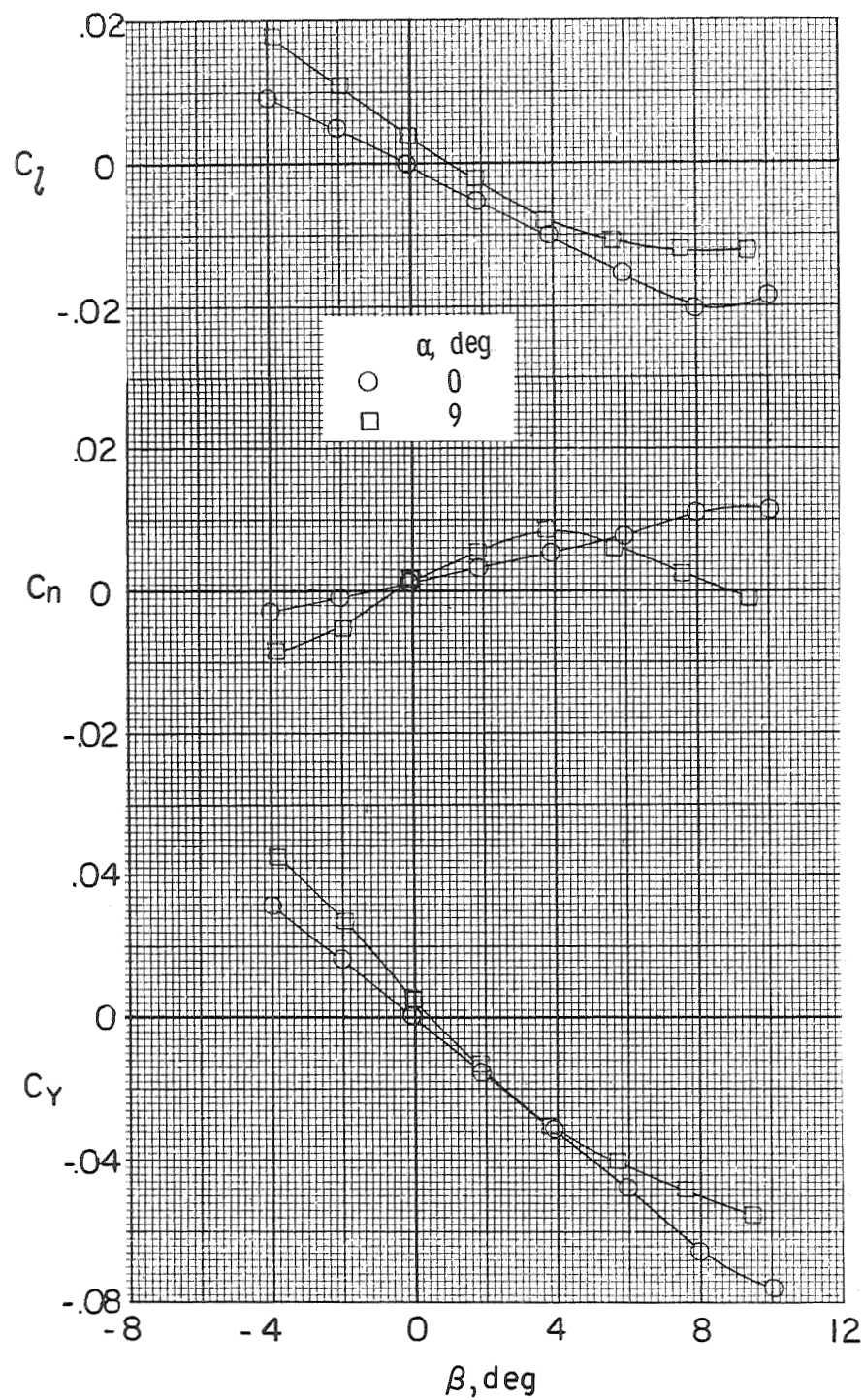
(d) C_m and L/D as functions of α .

Figure 9.- Continued.



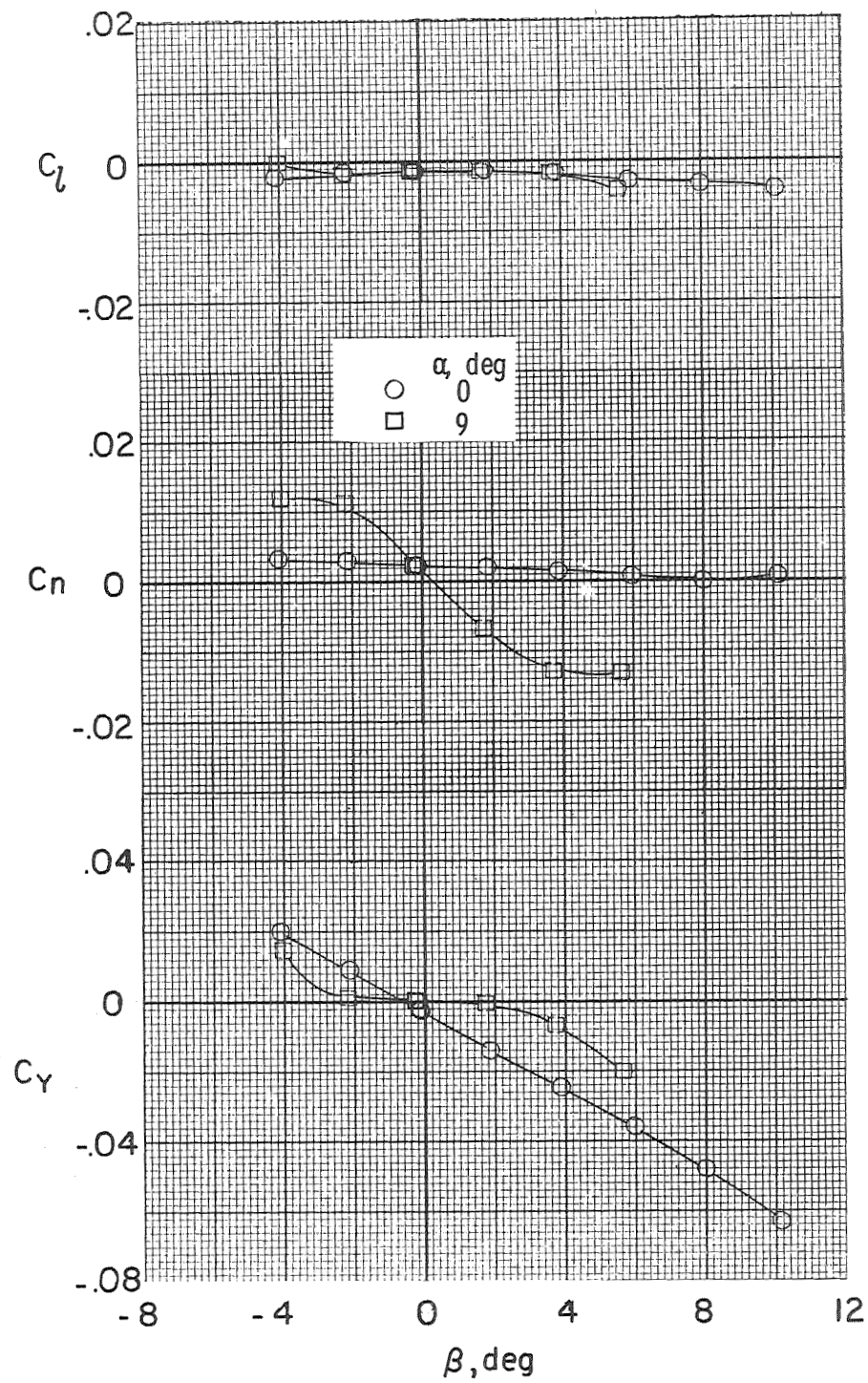
(e) C_m and L/D as functions of C_L .

Figure 9.- Concluded.



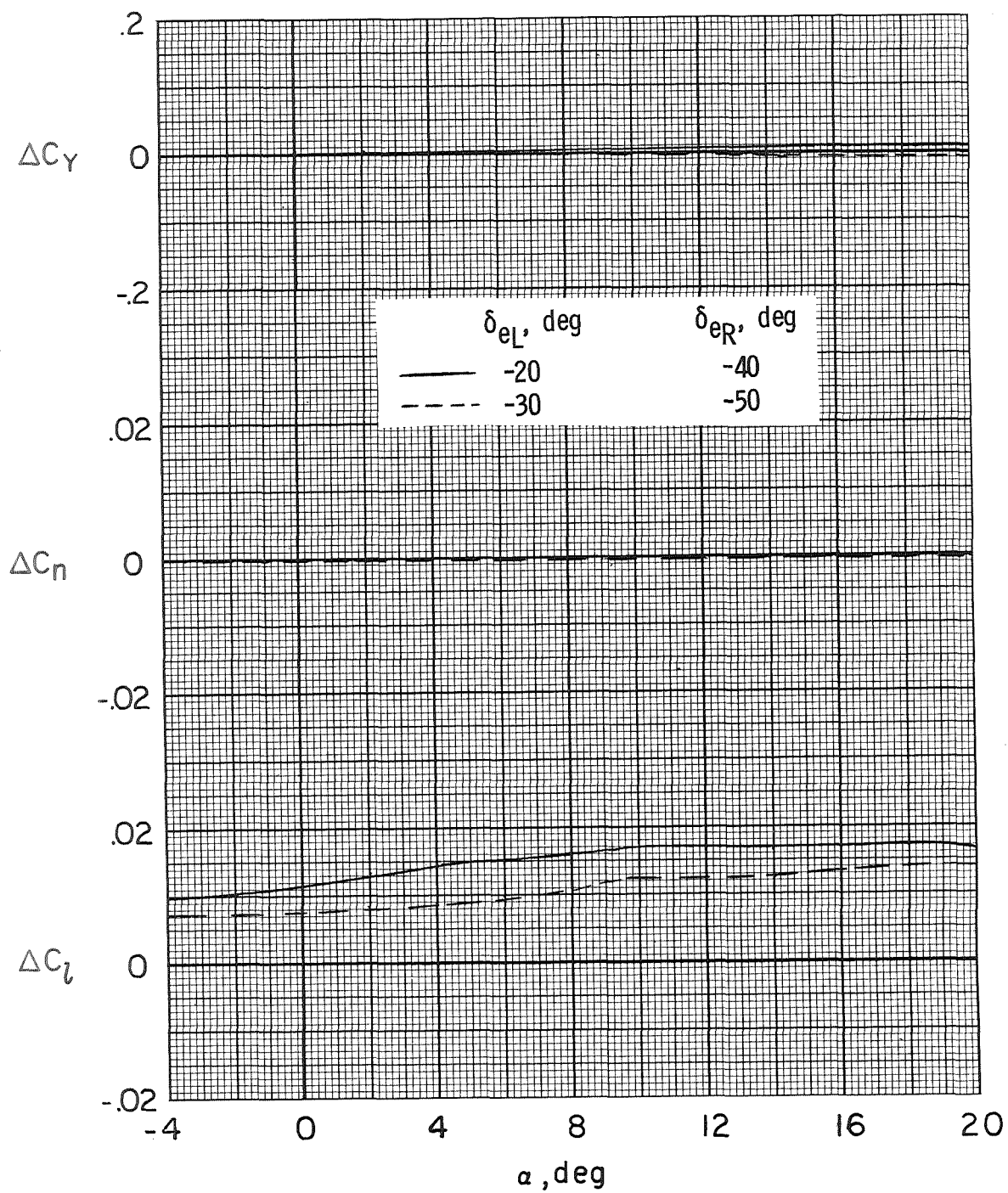
(a) $M = 0.4$.

Figure 10.- Static lateral stability characteristics of model. $\delta_e = 0^\circ$.



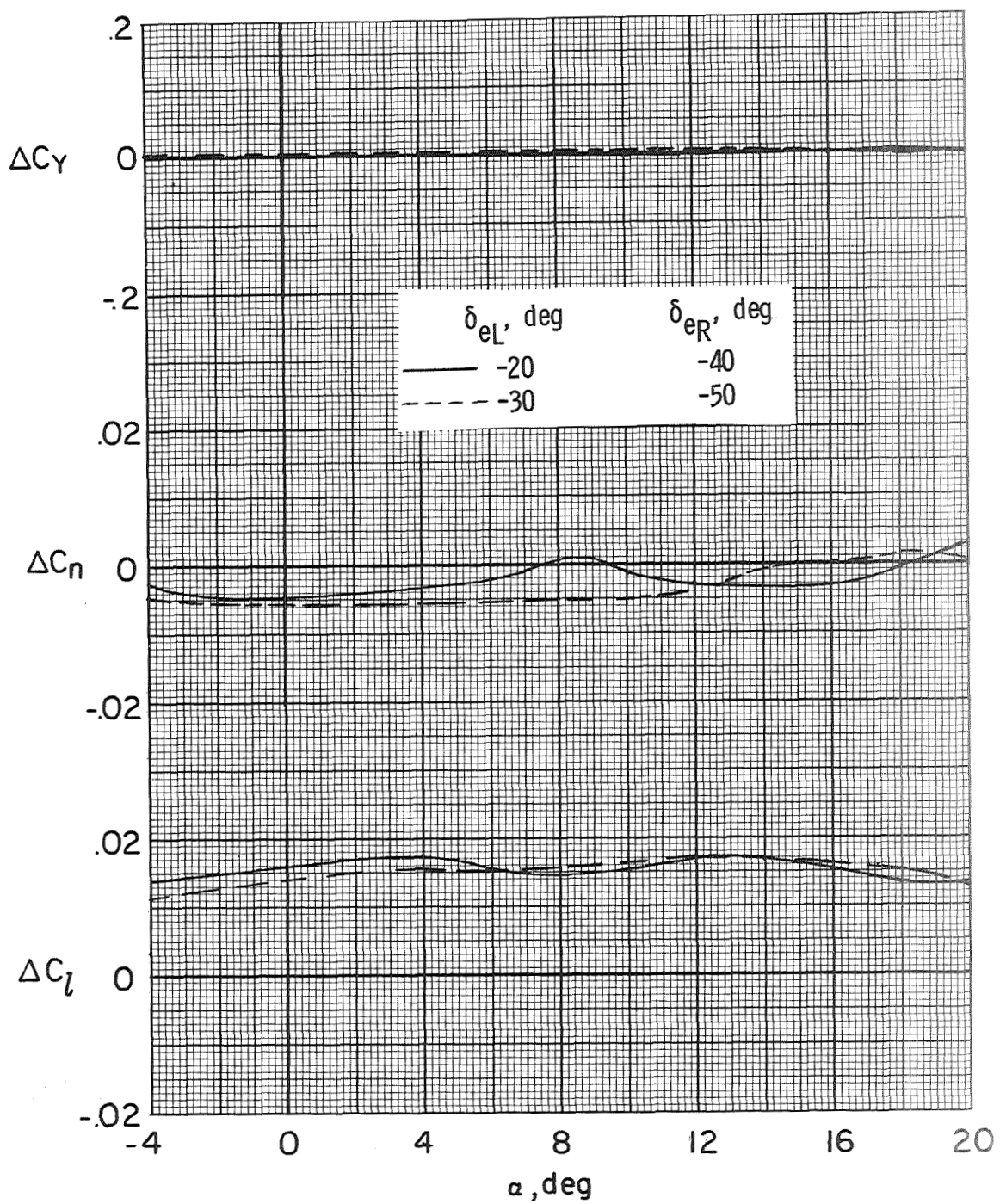
(b) $M = 0.8$.

Figure 10.- Concluded.



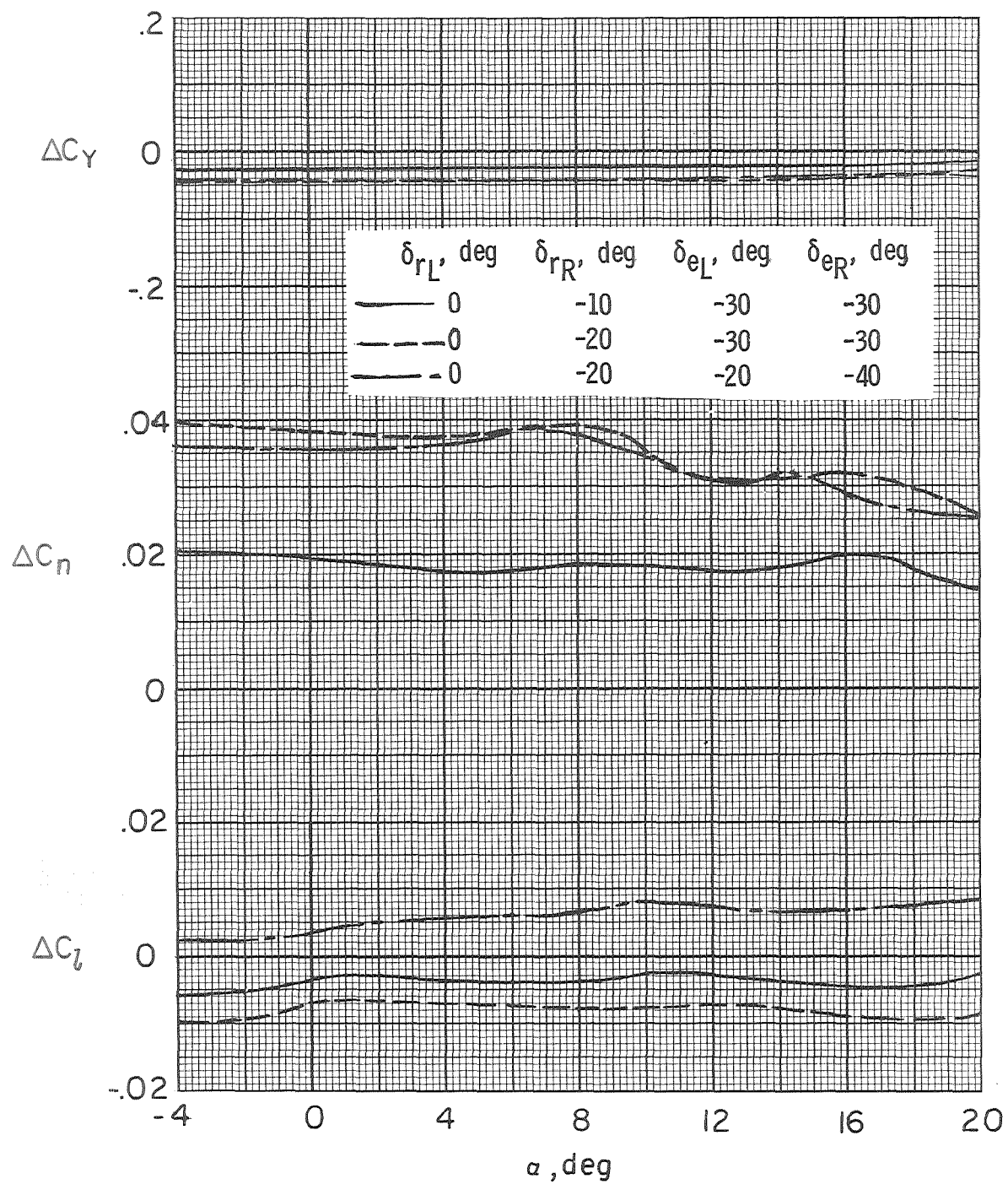
(a) $M = 0.4$.

Figure 11.- Roll-control effectiveness.



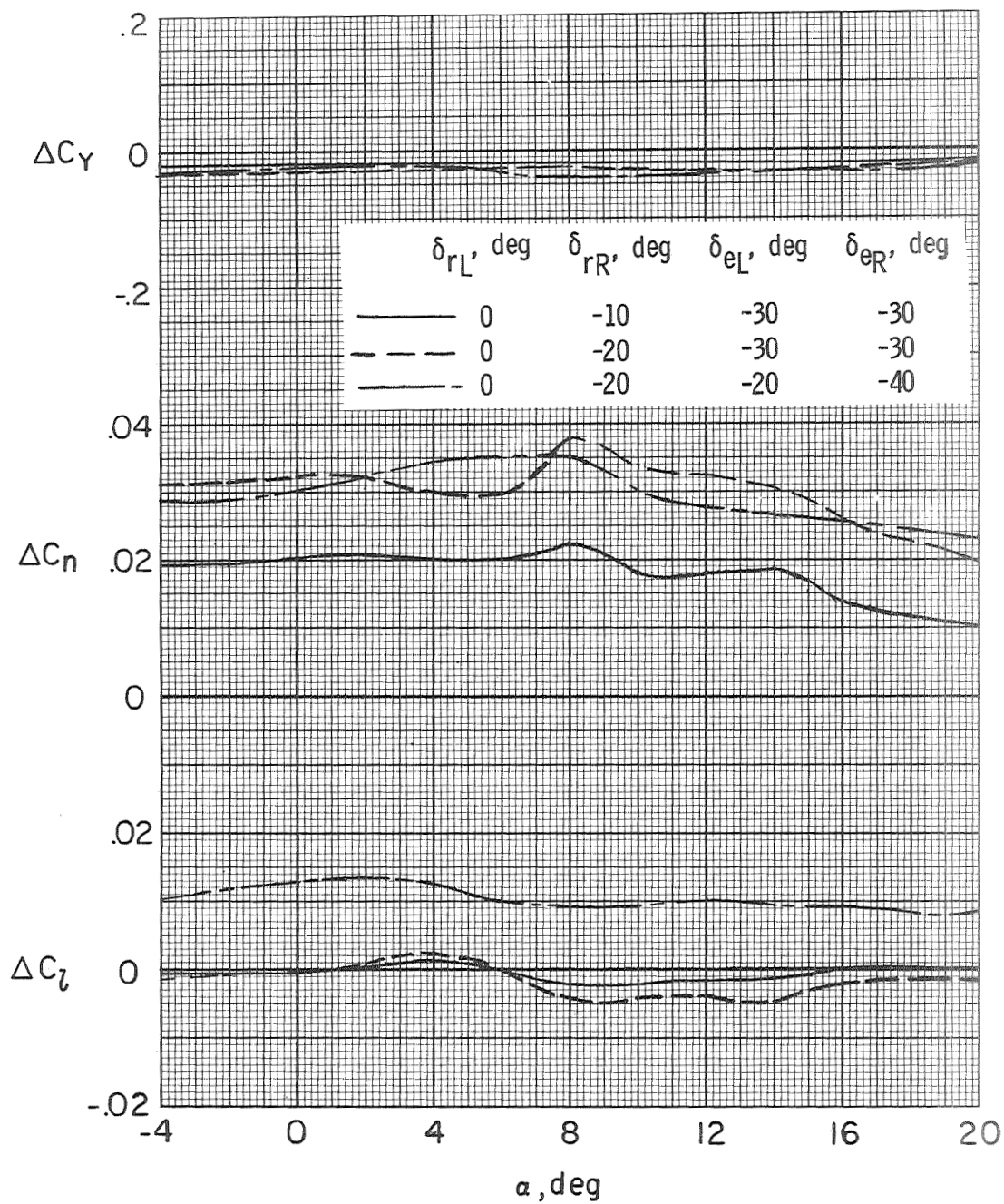
(b) $M = 0.8$.

Figure 11.- Concluded.



(a) $M = 0.4$.

Figure 12.- Combined roll- and yaw-control effectiveness.



(b) $M = 0.8$.

Figure 12.- Concluded.

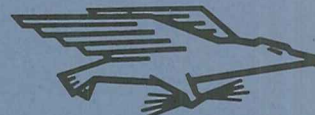
NATIONAL AERONAUTICS AND SPACE ADMINISTRATION

WASHINGTON, D.C. 20546

OFFICIAL BUSINESS

PENALTY FOR PRIVATE USE \$300

FIRST CLASS MAIL



POSTAGE AND FEES PAID
NATIONAL AERONAUTICS AND
SPACE ADMINISTRATION

POSTMASTER: If Undeliverable (Section 158
Postal Manual) Do Not Return

"The aeronautical and space activities of the United States shall be conducted so as to contribute . . . to the expansion of human knowledge of phenomena in the atmosphere and space. The Administration shall provide for the widest practicable and appropriate dissemination of information concerning its activities and the results thereof."

— NATIONAL AERONAUTICS AND SPACE ACT OF 1958

NASA SCIENTIFIC AND TECHNICAL PUBLICATIONS

TECHNICAL REPORTS: Scientific and technical information considered important, complete, and a lasting contribution to existing knowledge.

TECHNICAL NOTES: Information less broad in scope but nevertheless of importance as a contribution to existing knowledge.

TECHNICAL MEMORANDUMS: Information receiving limited distribution because of preliminary data, security classification, or other reasons.

CONTRACTOR REPORTS: Scientific and technical information generated under a NASA contract or grant and considered an important contribution to existing knowledge.

TECHNICAL TRANSLATIONS: Information published in a foreign language considered to merit NASA distribution in English.

SPECIAL PUBLICATIONS: Information derived from or of value to NASA activities. Publications include conference proceedings, monographs, data compilations, handbooks, sourcebooks, and special bibliographies.

TECHNOLOGY UTILIZATION PUBLICATIONS: Information on technology used by NASA that may be of particular interest in commercial and other non-aerospace applications. Publications include Tech Briefs, Technology Utilization Reports and Technology Surveys.

Details on the availability of these publications may be obtained from:

SCIENTIFIC AND TECHNICAL INFORMATION OFFICE

NATIONAL AERONAUTICS AND SPACE ADMINISTRATION

Washington, D.C. 20546